


ESCUELA TÉCNICA SUPERIOR DE INGENIEROS INDUSTRIALES Y DE TELECOMUNICACIÓN

Titulación :

INGENIERO INDUSTRIAL

Título del proyecto:

# DEVELOPMENT OF A STRETCHABLE AND IMPLANTABLE ELECTRODE ARRAY FOR MEASURING PERIPHERAL NERVE SIGNALS

Diego Marcos González

Jesús Corres Sanz

Pamplona, 25 de febrero de 2011

# Stretchable and Implantable Electrode Array for Measuring Peripheral Nerve Signals

Diego Marcos

Escuela Técnica Superior de Ingenieros Industriales y de Telecomunicación

UPNa

A thesis submitted for the degree of

*Ingeniería Insdustrial*

February 2011

Tutor in UPNa: Jesús Corres Sanz

Tutor in Fraunhofer IZM: Michael Zwanzig

# Abstract

As part of a collaboration project with the Department of Neurology at the University of Regensburg and the Institute of Biophysics at the University of Rostock, stretchable and implantable electrodes have been developed, aimed to obtain electric signals from peripheral nerves. These signals could serve for limb amputees to control a prosthetic device. Gold has been used for the electrode surface and the conductive paths, which are embedded in a stretchable Polyurethane foil. Three separated electrode heads, with two electrodes each, can be located on the free surface of a peripheral nerve. In order to increase the signal yield and improve the signal-to-noise ratio, the electrode surface has been covered with a micro-nano crystalline gold layer (Shark-teeth gold).

# Agradecimientos

Este trabajo, aunque sacado adelante principalmente con mis manos, ha requerido de las ideas y la experiencia de todos aquellos a los que he tenido que recurrir o me han ayudado espontáneamente, que han sido muchos. Empezando por mi tutor, Michael Zwanzig, y su colega Ralf Schmidt, que junto con Nuray Çilingir han estado conmigo todos y cada uno de los muchos días que he dedicado a este proyecto, y con los que he tenido el placer de discutir hasta el más nimio de los problemas que me han surgido. Pero están lejos de ser los únicos, pues un sinfín de empleados, tanto del Fraunhofer IZM como de la TU Berlin han prestado atención a mis preguntas en rudimentario alemán: Nuray Çilingir, Georg Rettner y Evelin Prochnow me han enseñado a moverme en el laboratorio de química; René Jansen y Manuel Seckel estuvieron conmigo en mis primeros pasos bajo los fluorescentes amarillos de la sala limpia; también Manuel Seckel, Stefan Karaskiewicz y David Schütze me enseñaron a manejar buena parte de los equipos que me resultarían imprescindibles. Aunque fueron muchos más lo que me ayudaron en momentos puntuales a lo largo de los más de 12 meses en los que hemos compartido un mismo edificio. Una mención especial se merecen Andreas Ostmann, director del grupo SIIT del Fraunhofer IZM, que intentó convencerme durante mas de 5 horas para que hiciera allí mi proyecto, cuando con 5 minutos hubiera sobrado; Vera Schmitt, de recursos humanos, que además de salvarme de la burocracia alemana me obsequió con horas de charla distendida pero apasioanda; Alexander Wirth, estudiante que me relevará en el proyecto E-Nerv cuando yo deje de dedicarme a él y quien, junto a Philipp Wachholz y Lu Huang, ha hecho que estos meses hayan sido aún más agradables. También quiero agradecer a mi tutor en la UPNa, Jesús Corres, por su apoyo y confianza.

Y puesto que este último año no ha sido sólo trabajar para el proyecto, me gustaría agradecer de corazón a los amigos que han iluminado las largas noches berlinesas de 16 horas, muy especialmente a mis compañeros de piso: Anne, David, Marion y Yann, que me han hecho acabar cada jornada con ilusión de llegar a casa.

Pero más importante que todo esto ha sido el apoyo incondicional que me ha dado mi familia desde Pamplona en todo momento, sin el que nada de esto habría sido posible.

# Contents

# 1 Introduction

## 1.1 The ENerv Project

This work has been written as part of a collaboration project between four German institutions:

- Research Center for Microperipheric Technologies at the TU Berlin
- Fraunhofer IZM in Berlin
- Department of Neurology at the University of Regensburg
- Institute of Biophysics at the University of Rostock

The project name in German is: *Elastisches Elektrodenarray zur Signalkopplung an periphere Nerven* (Elastic Electrode Array for Measuring Peripheral Nerve Signals) (1) but is commonly referred as ENerv. The kick-off was on July the first 2009 and was intended to last for 17 months until end of 2010, with a budget over 300.000 euro funded by the German Ministry of Education and Research.

The aim of the project is to determine the feasibility of an implantable multichannel ((2)(3)) electrode for measuring nerve signals from peripheral nerves or nerve stumps. Connected to a wearable computer, the objective is to use it for controlling prosthetic and orthotic devices. An additional requirement is that the electrode array has to be economic, what restricts the use of certain expensive technologies, like using silicon wafer as substrate.

Comparison with other approaches:

- Brain-computer interfaces require more complex data acquisition and processing systems.

- Muscle-computer interfaces can only be applied when intact muscles are present, which is not always the case.

The initial experiment was devised to consist of three parts:

- Development of nanostructured electrodes to achieve a reliable contact with the peripheral nerve tissue.
- Insert the electrodes in model animal for a period of several months, around the sciatic nerve of rats.
- Evaluation of the electrodes regarding the biocompatibility and long term reliability of the electric signal provided.

The present work covers most of the first point.

The project partners have to provide the necessary know-how after those steps have been covered: signal acquisition though an intracorporal electronic interface, signal treatment, analysis and conversion (local or external), wireless signal transmission, energy supply and actuators control. Additional contacts with the industry are foreseen with the aim of transforming the developed technology in a functional, ergonomic and attractive prosthesis.

## 1.2 Principles of the main processes

### 1.2.1 Silver immersion plating

Immersion or displacement plating is the deposition of a metal layer from a metal-ion solution on a metallic surface. The surface must have a lower oxidation potential, what triggers a redox exchange reaction where the metal ions in the solution are reduced by the metal of the surface.

In the case that concerns us, a silver solution is used for coating a copper surface. Copper is displaced by silver by the following reaction:

$$Cu + 2Ag^{+} \Rightarrow Cu^{2+} + 2Ag$$

The reaction continues until the whole copper surface is covered by silver, as then the source of electrons is isolated from the silver solution. For this reason only thin coatings can be achieved by this method. (4)

For this project a homogeneous and very thin coating was desired, as the thicker the silver layer the more difficult is to etch it away. It made immersion plating the best option, which also adds that it does not need a current source and does not require cyanide containing solutions.

In order to obtain optimal results, a commercial mix of chemical compounds has to be added to the silver solution that alters the properties of the plated silver layer.

### 1.2.2 Gold electroplating

To obtain the gold structures, gold will be deposited in the structured gaps of the developed photoresist through electroplating. Gold is present in the electrolyte in a monovalent form as $KAu(CN)_2$. In the electrolytic cell a platinised titanium grid will be used as anode, and the cathode will be the sample to be plated. When the current source is switched on, positive ions will be attracted to a region around the cathode, called the Helmholtz layer, which in turn attracts the negative complex ions of the surroundings, like $Au(CN)_2^-$, polarising them. When these ions reach the Helmholtz layer, they break up and the freed metal is deposited on the cathode. The physical distribution of the deposited metal depends on the characteristics of the Helmholtz layer, which can be controlled by several methods, like the addition of organic compounds, other metal co-deposition or controlling the pH value, temperature and current density. (5)

### 1.2.3 Photolithography

Photolithogrphy is used in the integrated circuits industry to transfer patterns onto thin films. Traditionally a mask has been placed between a light source and the wafer or circuit board that has been previously coated with a light sensitive film. Nowadays, in research environments where high flexibility is required, Laser Direct Imaging (LDI) systems are substituting the processes that involve the use of photomasks.

### Laser Direct Imaging

In LDI printing systems, a laser is used to directly transfer a pattern onto a photosensitive surface. Commonly a computer controls the focused laser beam through a collection of mirrors and lenses, raster scanning the surface. This eliminates the need of a mask, saving process time and costs, as well as avoids defects caused by wearing of the mask. LDI allows inexpensively changing the pattern design, offering a very high flexibility.

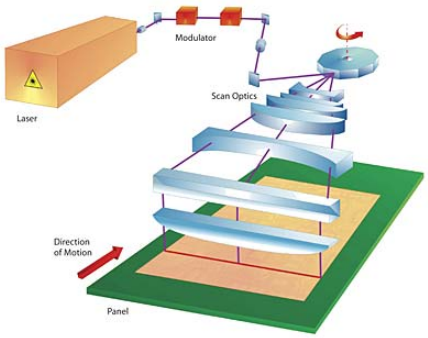


**Figure 1.1: Schematic of a LDI system** - Courtesy of Orbotech Ltd, Yavne, Israel

An Orbotech Paragon 9000 LDI system was available for this proyect. 1.5.1

### Positive Photoresist

A positive liquid photoresist was used for one of the gold structuring steps. The positive tone means that the exposure to a near UV light renders the coating soluble to mildly alkaline soutions, which can be used as developer, removing the areas of the sample that have been exposed to light. The unexposed resist can be dissolved in a strongly alkaline solution, typically a 3 to 5 % KOH solution.

In liquid resist the photosensitive polymer comes dissolved in some kind of solvent that provides the required viscosity for the spinning process. It consists in dispensing the liquid resist over the center of a spinning sample, over which the resist is homogeneously coated by action of the centrifugal forces that expel it outwards. The resulting polymer thickness is mainly function of the spin speed and the kinematic viscosity of the solution:

$$T = \frac{KC^{\beta}\eta^{\gamma}}{\omega^{\alpha}}$$

Where K is an overall calibration constant, C the concentration of polymer in the solution and $\eta$ the viscosity. $\alpha$, $\beta$ and $\gamma$ are parameters determined experimentally. (6)

For this work the positive photoresist Clariant AZ 4562 was used. 1.5.2

**Negative Photoresist**

Using a negative resist, the mask has to be inverted in order to obtain the same result as with a positive resist. It usually consists of a polymeric material soluble in a mildly alkaline developer. The areas that are hit by light undergo a polymerization process that renders the material more stable and non soluble in the developer solution.(6)

For this work the negative photoresist Hitachi RD 1225 was used. 1.5.2

## 1.3 Nerve Signal Sensing

### 1.3.1 Introduction

The signal transmission system in living nerve tissues is based on a series of complex chemical processes.

The possibility of intercepting this signals through measuring the subsequently generated electric charges has been long known, but it is still a technical challenge to develop an effective man-machine interface, combining separated disciplines such as robotics and prosthetics, to allow controlling devices directly by thinking.

### 1.3.2 State-of-the-Art

Development in the fields of prosthetics can be represented by the bionic hand (7) built by van der Smagt and Bitzer, respectively from the German Aerospace Center and the University College London. It is a prosthetic robotic hand that is controlled using an electromyographic (8) (EMG) interface and, therefore, requires the presence of muscles in the forearm in order to collect the users signal. This system is not useful

for amputees who have lost these muscles or have them damaged. Such patients would require a system obtaining the signal directly from the nervous system, through the so called Brain-Computer Interfaces (BCI). It can be done with techniques of different levels of invasiveness:

- Non-invasive methods, like electroencephalograms (EEG), allow achieving only low resolution data (9) from which is mathematically impossible to calculate the actual intracranial activity (10). Other non-invasive technologies, like those based on magnetic resonance imaging or positron emission tomography, while offering a much higher spatial resolution are limited in terms of temporal resolution and need expensive and voluminous equipment.
- Invasive and semi-invasive methods collect the neural information from direct contact with the brain, the former from inside the brain tissue and the latter only from its surface, usually beneath the dura mater. Both require surgically inserting some kind of electrode inside the skull (11).

## 1.4 Stretchable Electronics

The concept of a chronically implantable electrode in a limb requires it to physically adapt itself to the changing topography of the surrounding muscles. For this purpose, we used the know-how in stretchable electronics developed in Fraunhofer IZM and TU Berlin in the framework of the EU project STELLA (12), for which a process was designed to embed a copper circuit in a thin polymer matrix in order to interconnect several rigid electronic parts with an stretchable support. To increase the stretchability of the metallic part of the circuit, a meander shaped copper path was used(13), method that was directly imported into the E-Nerv circuit design. The polymeric matrix material used in this project, Walopur®thermoplastic polyurethane (TPU) provided by Epurex, and most of the parameters of the embedding process had also been taken from the experiences with copper stretchable circuits. Due to dimensional demands of the application, the E-Nerv project would need smaller structure sizes than STELLA (25 $\mu$m line width compared to 100 $\mu$m line width in STELLA) and gold circuits instead copper, what would require deep modifications in the process parameters.

## 1.5 Resources

For this work around €2000 in material expenses were foreseen, as well as access to the required equipment available in both Fraunhofer IZM and the Technical University in Berlin.

**Fraunhofer IZM** The Fraunhofer Society is a German application-oriented research organization, with over 60 institutes around the country and €1.7 billion of yearly budget in 2010. The Fraunhofer Reliability and Microintegration Institute (IZM), based in two locations in Berlin, as well as in Munich, is specialized in microelectronic and microsystem technologies. In 2009 it had 251 employees and a turover of €27 million.

**TU Berlin** The Technische Universität Berlin (Berlin Institute of Technology) is, with 30.000 students, one of the biggest universities of Germany. In 2010 it was ranked 48th in the world in the field of engineering by the Times World University Ranking.

### 1.5.1 Equipement

**Chemistry laboratory** Facilities located at Fraunhofer IZM in the Technology and Innovations Park Berlin (TIB).

- Electroplating equipment, using a Keithley 2400 SourceMeter as current source.
- Optic microscopy up to 1000x.
- X-ray spectroscopy for layer thickness measurements and elemental analysis.

**Substrate Technologies laboratory** At Fraunhofer IZM in the TIB. Most equipement available is specialized for big surface electronics.

- Laser Drilling Machine Siemens Dematic MicroBeam 3200, for laser ablation, drilling and cutting (Fig 1.3 b).
  - 355 nm diode puemped solid state laser (vanadate).
  - Average power 3.5 W at 20 KHz.

**Figure 1.2: Electroplating equipement** - Gold electroplating with Keithley 2400

  - Pulse with of 35 ns at 20 KHz.
  - Spot size around 15 $\mu$m.

- Lauffer LC 40 / 2E HATVacuum PCB-Laminating Press System, for substrate embedding (Fig 1.3 a).

a) 

b) 

**Figure 1.3:** - Lauffer PCB-Laminating Press (a) and Siemens Dematic MicroBeam 3200 (b).

- LEO 1540 Cross Beam Field Emission Scanning Electron Microscope and FIB Workstation.

  - SEM resolution: 1 nm at 20 kV.
  - Magnification 12 to 900k.
  - Focused Ion Beam to section small samples.


**Figure 1.4:** - Cross Beam Field Emission SEM and FIB Workstation

- Fischerscope®XRAY XDV-SD, X-ray spectroscopy for thickness measurement.

**Photo-lithography laboratory** in a 800 $m^2$ clean room environment, classes 10 to 1000, at TU Berlin in the TIB.

- Laser Direct Imaging Orbotech Paragon 9000, for printing on photo-sensitive resist (Fig 1.5 a).
  - Laser source: 8 W DPSS 355 nm.
  - Data resolution: 2.5 $\mu$m.
  - Minimum feature size: 15 $\mu$m.
  - Exposure range: 10 - 2000 mJ/$cm^2$.
- Laurell Technologies, Co. spin coater (Fig 1.5 b).

- Dry resist lamination press (Fig 1.5 c).
- Schmid Inline spray resist developer (Fig 1.5 d).

a) b)

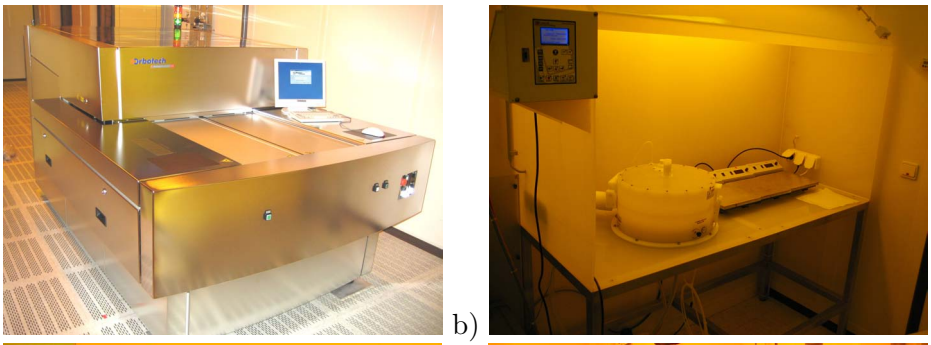

c) d)

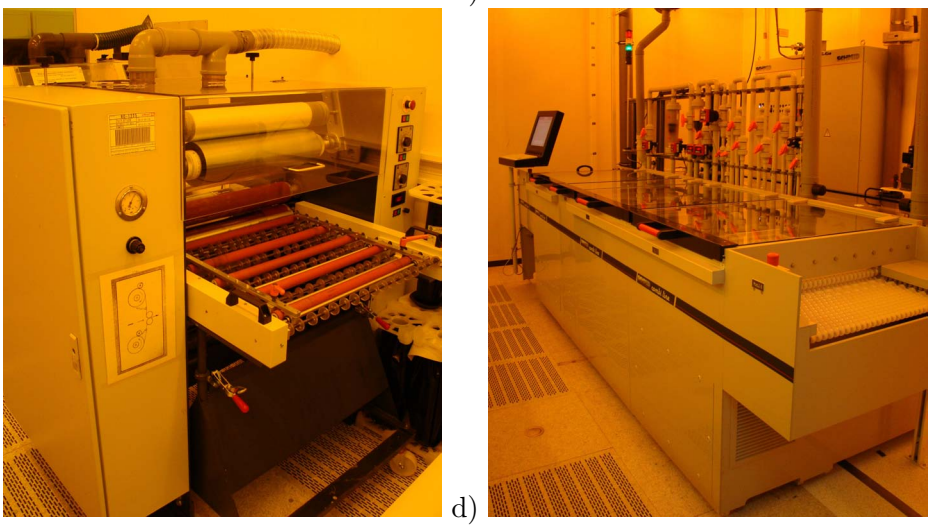

**Figure 1.5: Main equipement in clean room facilities** - Orbotech Paragon 9000 (a), spin coater (b), laminator (c) and inline developer (d).

### 1.5.2 Materials

#### Photoresists

- AZ 4562

  The AZ 4562 liquid positive photoresist, manufactured by Clariant GmbH, allows single layer thickness of between 3 and 15 $\mu$m. It tends easily to overdevelop, what provides soft slopes in the developed polymer. While this effect is usually considered a problem to be avoided, it can be useful for our process, as the

subsequent electroplated structures would have a wedge shaped profile that could enhance their physical stability in the polyurethane matrix.

- RD 1225

  By Hitachi Chemicals, dry resist, intended for lamination, with a thikness of 25 $\mu$m. Provides clean sharp edges for up to 20 $\mu$m plated structures.

**Substrates**

- Walopur®AU 4201 25 $\mu$m Polyurethane by Epurex Films GmbH.
- Copper sheet 35 $\mu$m thick.
- Release Film ACC-3, PTFE-based by Holders Technology GmbH.
- Stiffener ACC-14 Holders Technology GmbH.

**Chemicals**

- Gold dicyanoaurate salt.
- Puramet 202 gold electrolyte by AmiDoduco GmbH.
- AlphaSTAR Immersion Silver by Enthone, Inc.
- Alkaline copper etching solution.

### 1.5.3 Team

More decisive for the smooth running of this project than the resources already mentioned is the knowledge with which the team at Fraunhofer IZM and the Berlin Institute of Technology contributed to it, mainly in the fields of microtechnology, materials science, chemistry and biology.

# 2

# Premises and objectives

This thesis was developed on the part of the ENerv project assigned to the TU Berlin and the Fraunhofer IZM, and its scope covers the search for the optimal parameters needed to build the first functional prototypes of the electrode, given a predesigned concept (Fig. 2.1) for such a process. Although some of the presumably needed sub-processes had been extensively tested in house, there are some others that would present important technical challenges.

**Proposed layout:** (Fig. 2.1 a) The electrode was designed to provide contact to 3 spots on the nerve surface, with 2 neighbouring contacts in each spot. The signal has to be transferred through a meander shaped path to the contact pads on the other end of the electrode, which is 53 mm long. The tip (1) that has to be in contact with the nerve is reinforced with an arrow-shaped gold sheet to improve stability and adhesion to the tissue. The two circular pads behind the tip arrow are to establish contact with the nerve tissue. The back pads of the electrode (2) are envisioned to be used for a single measurement and then to be cut away. The four rows of pads would allow performing four measurements with each electrode. A bigger pad (3) connects all the conducting parts of the electrode together to simplify the electroplating process required as last step for nano-structuring the surface of the contact pads at the tip of the electrode.

**Proposed process:** (Fig. 2.1 b) One side of a 35 $\mu$m thick copper is laminated with a photoresist, which is structured in a LDI system and developed, leaving free of resist the areas to be plated with gold. After the gold plating, a layer of polyurethane is laminated over the gold structures, and the copper is etched away. A second PU lamination is performed to completely enclose the gold structures. Holes are drilled in the PU to set free the gold area that is to be contacted, and the hollow is filled by gold plating that leaves a nano-structured surface. Finally, the PU is cut to give the right shape to the electrode.

a)

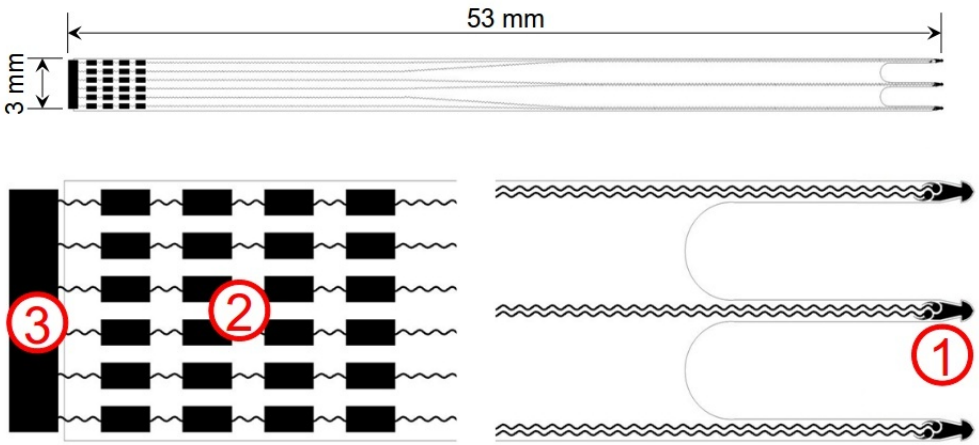


b)

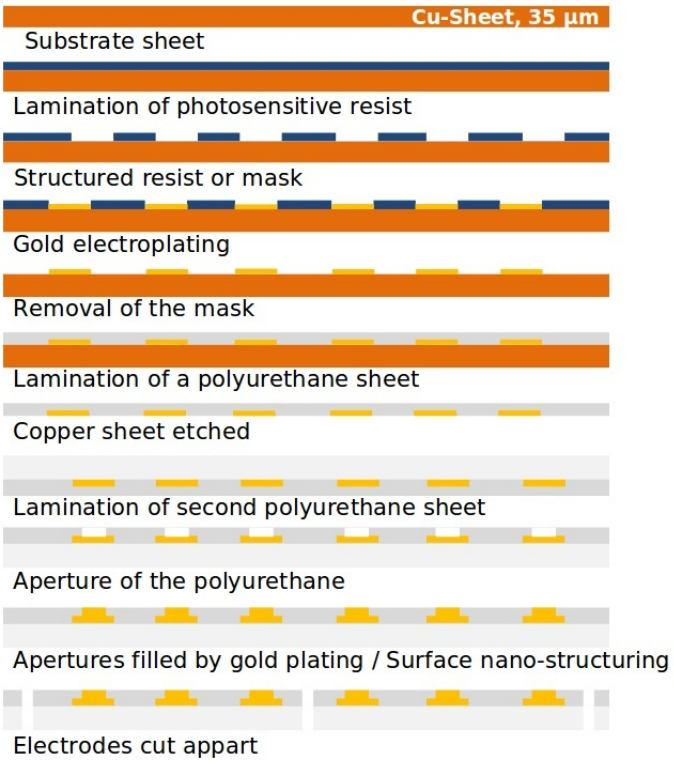


**Figure 2.1: Status at the beginning of this work**

## 2. PREMISES AND OBJECTIVES

As of the start of my stay in the Fraunhofer IZM, the E-Nerv project had already run for some months. The initially proposed process flow had already been tested and it was shown that several more months of research would be needed to obtain functional electrodes. Most of the problems were related to the unusually small scale, 25 $\mu$m in width, of the gold conductive path used to transport the signal together with the stretchable nature of the whole electrode. Obtaining a continuous conductive path, without breaks, as well as a method to create a stable contact interface with the nerve tissue, seemed to be most important challenges to face. In the project timeframe, from October 2009 to December 2010, we needed to develop the process capability to manufacture enough functional electrode prototypes to provide with the other project partners in a way that they can determine the feasibility of the approach and decide whether it is worthy or not to extend and fund the E-Nerv project further.

# 3

# Development and Discussion

In this chapter the evolution of each step of the electrode fabrication process is explained. Partial results of these technological steps are also discussed.

## 3.1 Electrode layout

We started using 13x13 cm plates with 26 electrodes in each one, using the design originaly proposed in the kick-off meeting, as seen in Fig. 2.1 (a).

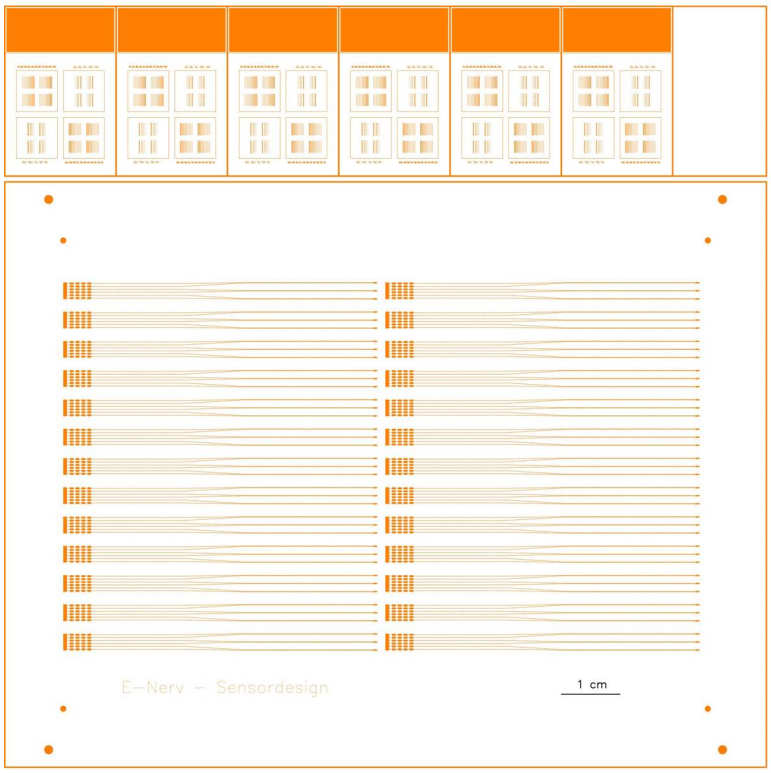


**Figure 3.1: First electrode layout design** - Additional to the 26 electrodes, six small test samples were printed. The circles near the corners are fiduciary markers.

After some first tests, we concluded that the conducting paths should be narrower,

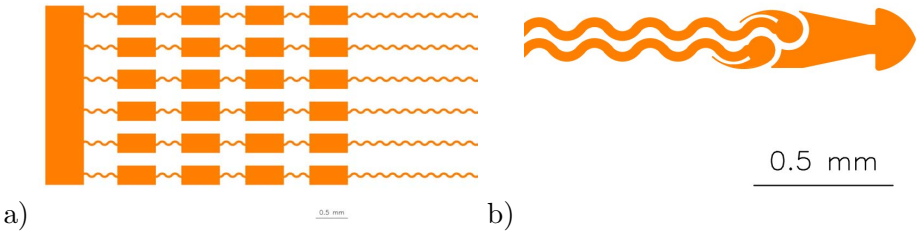


**Figure 3.2: Details of the first design** - Rear side of the electrode, with several contacting pads (a), and the tip, with the nerve contacts and the arrow-shaped stabilizer (b).

to compensate the tendency of the AZ photoresist to produce structures wider than designed. The stabilization arrow was made wider and a hole was opened in it to allow the surgeon to insert a needle for handling.

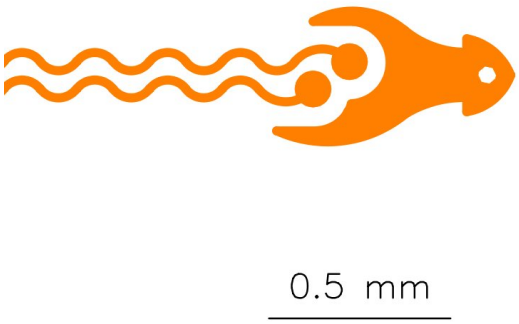


**Figure 3.3: Second version of the electrode tip** - Made wider and with a handling hole.

The electrodes on the right side of the panel were mirrored to locate all the tips, the most sensitive part of the electrode, in the middle of the panel, where it is less exposed to risks in the different steps of the production. Finally, the number of electrodes per plate was reduced to 24, in order to allow some smaller test designs to be printed in the same plate.

The first surgery test in Heidelberg with this design showed that the hole in the stabilization sheet, of just 60 $\mu$m in diameter, was far too small and that the extra width

given to this structure could cause problems. It was also decided that the contacts should be in-line and have a bigger distance between them (from 150 $\mu$m to 1000 $\mu$m centre to centre). The length where the distance between paths was minimal was reduced from some 2 cm to 3 mm, in an attempt to reduce parasitical currents between paths. The connection area between the path and the contact pads at the back end of the electrode were reinforced with a stabilization structure.


**Figure 3.4: Detail of the final electrode layout design** -

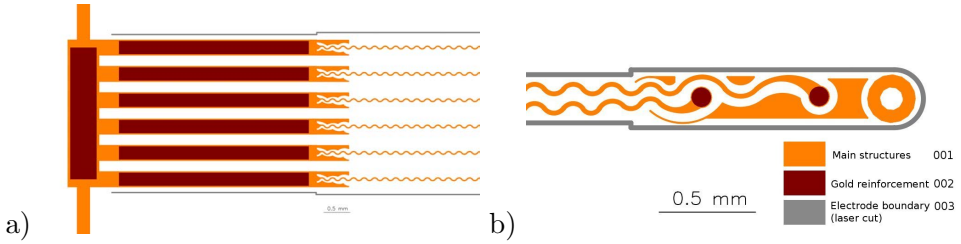


**Figure 3.5: Details of the final design** - Rear side of the electrode, with several contacting pads (a), and the tip, with the reinforced nerve contacts (b).

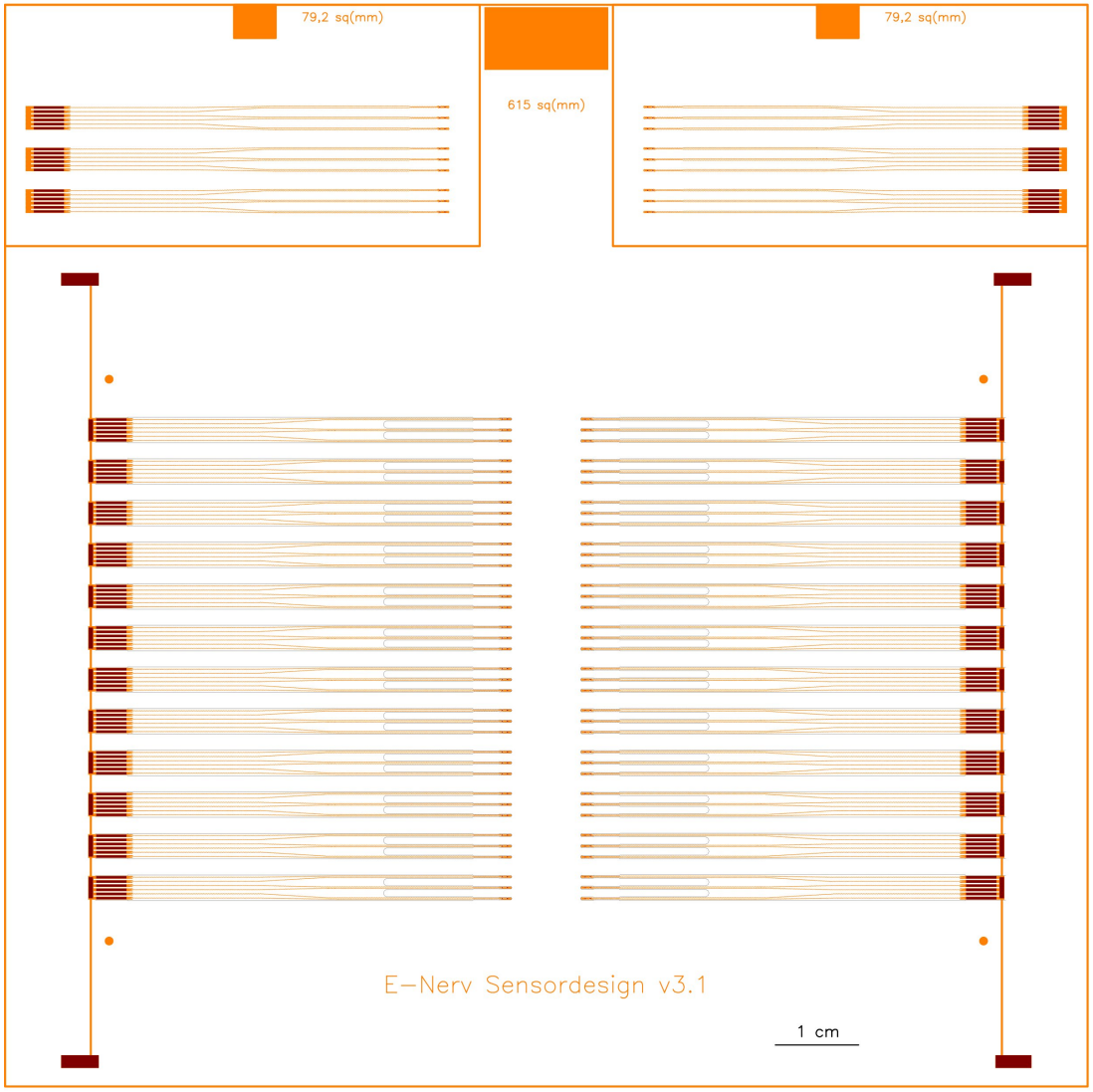


**Figure 3.6: Final electrode layout design** - Additional to the 24 electrodes, two sets of three electrode test samples were printed. The circles near the corners are fiduciary markers.

## 3.2 Immersion Silver

### 3.2.1 Introduction

Even at room temperature, the diffusion rate of copper through a copper-gold interface is high enough to affect the resistivity of the gold conductor(14), and this could also, presumably, reduce the biocompatibility of the electrode due to the toxicity of copper. It has also been observed that the silver plating of the copper surface improves the adhesion of the dry film photoresist that will be needed further in the process, reducing the risk of delamination during the gold electroplating (see Section 3.4), where it also reduces the risk of copper contamination of the gold electrolyte. These reasons led to the decision of coating the copper foil substrate with a thin (around 200 nm) layer of metallic silver. The immersion silver Sterling from MacDermid, Inc. was used.

### 3.2.2 McDermid Ag Immersion

The copper foil is cut in 30x35 cm rectangles, which will be split into four 15x15 squares after the chemical silver treatment. The residual 5x30 cm rectangle is used to handle the sheet and has to be discarded as some oxidation appears around this area. Initially a 70 $\mu$m thick copper foil was used because it has to be completely removed afterwards, and a thicker layer would consume more time and etching solution. However, the handling of such a thin sheet was problematic, and severe crumpling tended to occur (Fig. 3.7). Therefore a 105 $\mu$m thick copper foil was finally chosen, as the stiffness improvement simplified the handling and the crumpling problems were almost eliminated.

The process used was the standard for silver coating used at the IZM:

- Acid Cleaner: 1 min; 55C
- Wash in de-ionized water
- Microetch Silver: 1:30 min; 35C
- Wash in de-ionized water
- MacDermid Ag Predip: 0:30 min, 35C

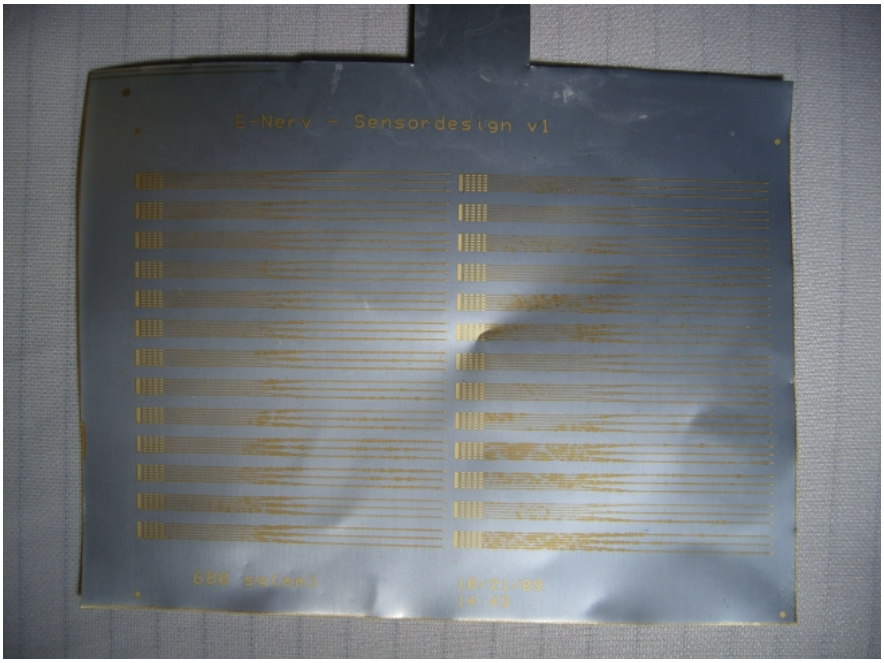


**Figure 3.7:** - Crumpling in 70 um thick sample

- MacDermid Ag Immersion: 2:00 min, 55C
- Wash in de-ionized water
- Dry with nitrogen

Washing immediately after the acid cleaner bath is important to minimize oxidation of the copper surface. Drying fast with a nitrogen jet after the last step is preferred to natural evaporation because it also reduces the risk of silver oxidation.

The copper sheets we used were stored in a standard room environment and were affected by airborne contamination. Contamination particles in the copper surface were found to remain stable during the whole process, possibly affecting the silver deposition over a small area around them. This could leave a small hole trough the silver coating under the particle, where the copper starts to oxidize, generating a red halo around the particle, effect known as red plague (15) (Fig. 3.9). It has been proved that those particles, as well as the disturbed area around them can prevent the gold deposition, ruining the whole structure (Fig. 3.8).

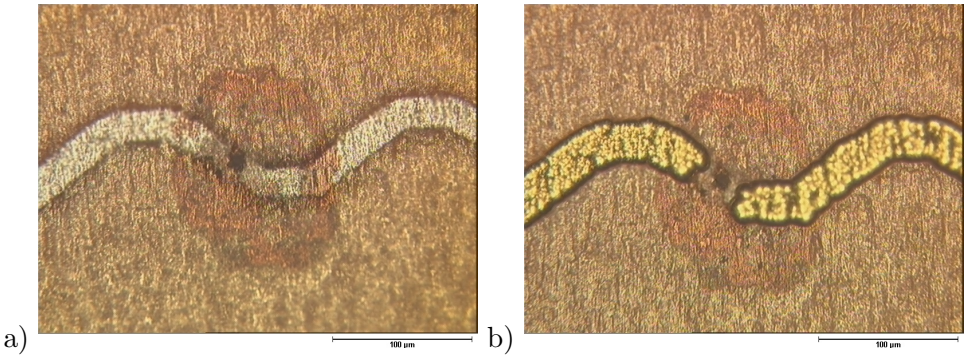


**Figure 3.8: Disturbed areas around particles** - Area of the silver plated copper foil structured with AZ photoresist affected by a particle: before gold plating (a) and after gold plating (b), where a break in the gold path can be seen.


**Figure 3.9: Red Plague** - Stain that usually can be found under disturbed gold structures.

We could notice that dipping the cooper foil for 5 minutes in a 5% KOH bath at room temperature previous to the acid cleaner achieved to remove most of the observed particles. This measure, combined with using a freshly prepared chemical silver immersion bath, still left an important amount of defects in the gold surface,

but almost all of them sharing the same characteristics: round pits of between 20 $\mu$m and 70 $\mu$m in diameter that can be identified as brighter regions under Differential Interference Contrast (DIC) microscopy (Fig. 3.10).

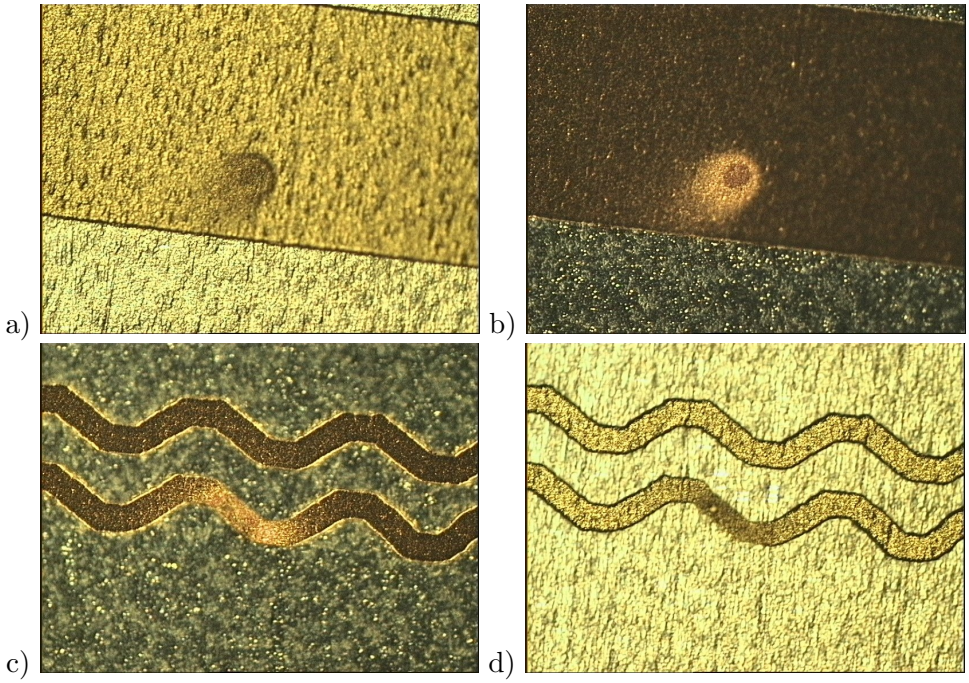


**Figure 3.10: Pits in plated gold due defects in the silver plating process** - Images taken by optical microscopy, (a) and (c), and DIC optical microscopy, (b) and (d), where the contrast of the failure is higher and can be detected more easily.

### 3.2.3 AlphaSTAR Ag Immersion

As copper cleaning procedures did not seem to improve the quality of the gold plated structures to the level we needed, we performed a gold plating test [See Silver plating test] over silver coated copper foil using four different combinations of two parameters for the silver plating: two different immersion silver suppliers (MacDermid and AlphaSTAR) and with or without an additional silver electroplating step. The test showed, on the one hand, that the 2 minutes long silver electroplating, with a resulting deposition of around 1.2 $\mu$m of silver, did not only not cover the flaws present in the first, electroless, plating, but also created some new ones. The pits in the gold layer caused by flaws in the silver immersion process tended to be round shaped, in the range

of 20 to 50 $\mu$m in diameter and of darker appearance under DIC microscopy (Fig. 3.11 a, b), while the pits caused by the silver electroplating had irregular shape, up to 100 $\mu$m long and bright under DIC microscopy (Fig. 3.11 c, d).

On the other hand, it showed clearly a much lower concentration of defects in the gold layer plated over AlphaSTAR silver, in comparison to MacDermid.

The first electrode samples built over AlphaSTAR silver coated copper showed a four fold improvement in acceptable electrode structures, having around 80% of the electrode conducting paths no spot affected by any kind of pit-like defect.

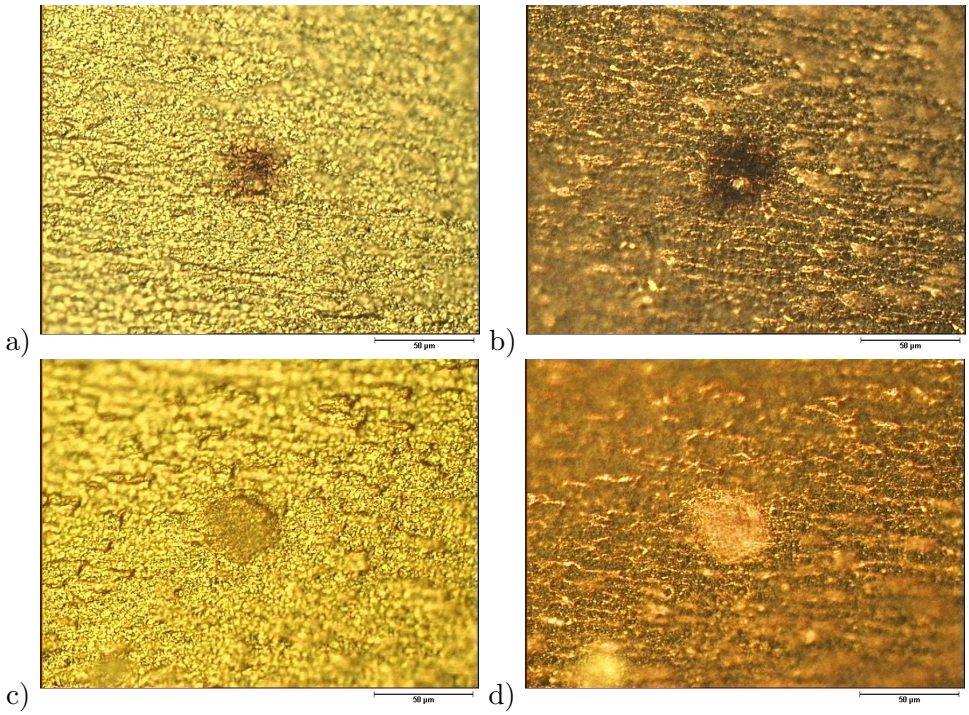


**Figure 3.11: Defects in plated gold due to defects in the silver plating process** - Stain on the gold plated layer over AlphaSTAR immersion silver (a, b). Pit on the gold plated layer over an electroplated silver surface (b, c). Images taken by optical microscopy, (a) and (c), and DIC optical microscopy, (b) and (d), where the contrast of the failure is higher and can be detected more easily.

## 3.3 Electrode structuring

### 3.3.1 Introduction

The first lithography step has to define the main structures of the electrodes, including the meander shaped conductive path, which consist in two 25 $\mu$m wide lines running together at an approximate distance of 30 $\mu$m. A LDI system (1.5.1) was used, allowing us to have a very high design flexibility (16).

### 3.3.2 KOLON resist

Preliminary tests with the negative dry photoresist KL-1015, manufactured by Kolon Industries, all resulted in non satisfactory results. On the one side, it was difficult to control the formation of photoresist bridges during the development process (Fig. 3.12 a). Due to the way the LDI system works, bridges were more likely to appear in vertical lines than in horizontal ones. These bridges prevented the gold from correctly building the structures (Fig. 3.12 b).

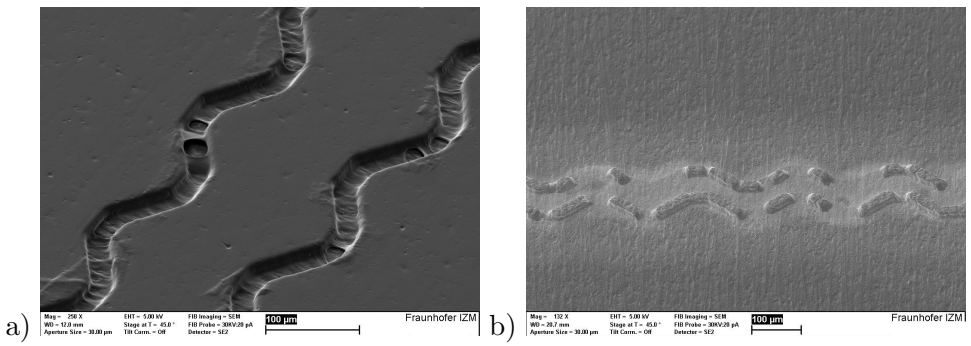


**Figure 3.12: Bridges through the structures due to defective development** - Right after development (a), and after gold plating and resist stripping (b).

On the other side, the resist showed some adherence and/or permeability issues, resulting in a halo looking area around the gold structures where a layer of up to 100 nm thick of gold covers the silver surface (Fig. 3.13). This effect depends strongly on the pH value of the gold electrolyte, which nominal value is from pH 5.5 to 6.5, with values between pH 5.7 and 5.8 giving the best results, but not yet halo-free.

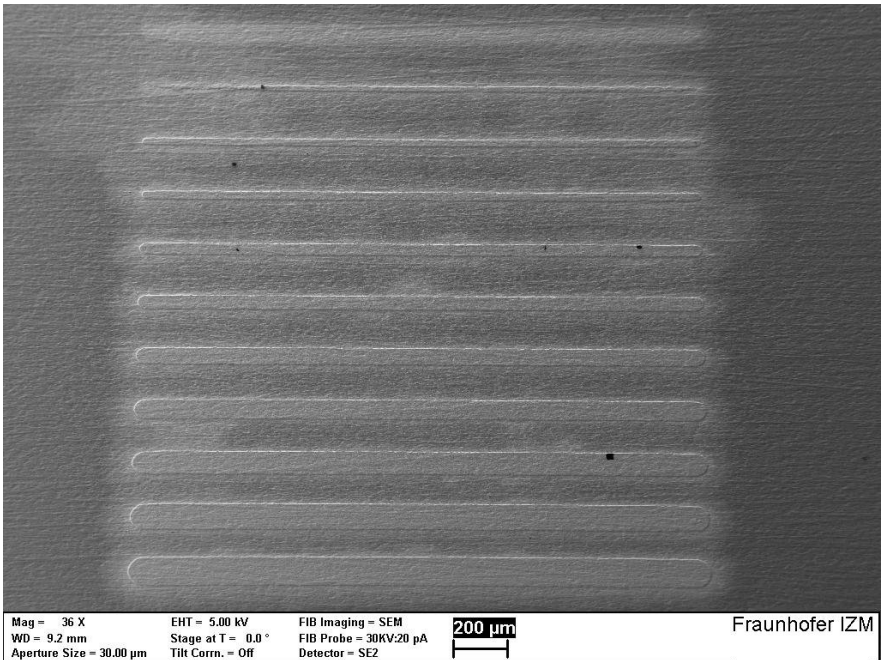


**Figure 3.13: Halo around the gold plated test lines** - A thin layer of gold short-circuits the gold structures

### 3.3.3 AZ-4562 resist

As next step, the positive liquid resist AZ-4265 was tested. The resist was spun over the silvered Cu foil with the standard AZ program and prebaked for 10 minutes at 100 °C. The exposition in the LDI was done at 450 mJ/cm$^2$, as specified by the manufacturer, and developed for 3 minutes at room temperature using AZ developer. The last step was to bake the samples at 130°C for 30 minutes. The first results showed a much better adherence of the resist anywhere in the nominal pH range of the electrolyte (pH 5.5  6.5), as no gold at all could be detected outside the designed structures (Fig. 3.14).

In order to avoid the backside of the sample from being completely plated with gold, what would be quite prohibitive, we covered it with galvanic tape. But removing it afterwards without damaging the sample was a very complicated and time consuming task. We eliminated the need of tape by laminating the back side after the hardbake with dry photoresist. To avoid damaging the AZ structures, they were covered by a clean room fabric tissue and the laminator roll contacting this tissue was left at room

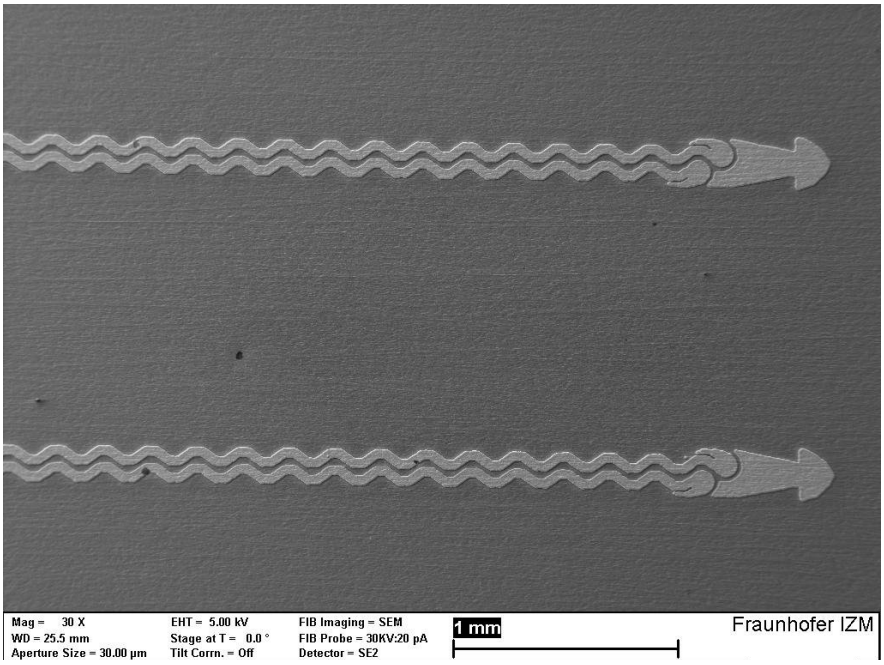


**Figure 3.14: Halo-free gold structure** - Plated using AZ-4562 photoresist

temperature, while the other was set to 110°C. The backside had to be then exposed in the LDI or by a UV lamp. We used a 300 W UV lamp, exposing each sample for 20 seconds. This did however bring some problems, as when removing the tissue some resist particles tended to come off and glue electrostatically to the AZ resist structures, blocking the proper growth of gold underneath (Fig. 3.15).

We decided to coat both sides of the sample with AZ resist, first the backside, in order to be able to clean the front side by spinning it with acetone before coating it.

Another problem was the clear overdevelopment caused by this process. Both conductive paths should be 25 $\mu$m wide and have a free space of 35 $\mu$m between them. In the image 3.16 can be clearly observed how the paths are wider than the gap between them.

A solution given by the manufacturer to this problem was to develop the samples in diluted AZ developer in 1:1 proportion with distilled water. The first test results to set the new development time suggested at least 8 minutes (6.1.3) in the diluted developer at room temperature with gently shaking by hand. Lower development times would

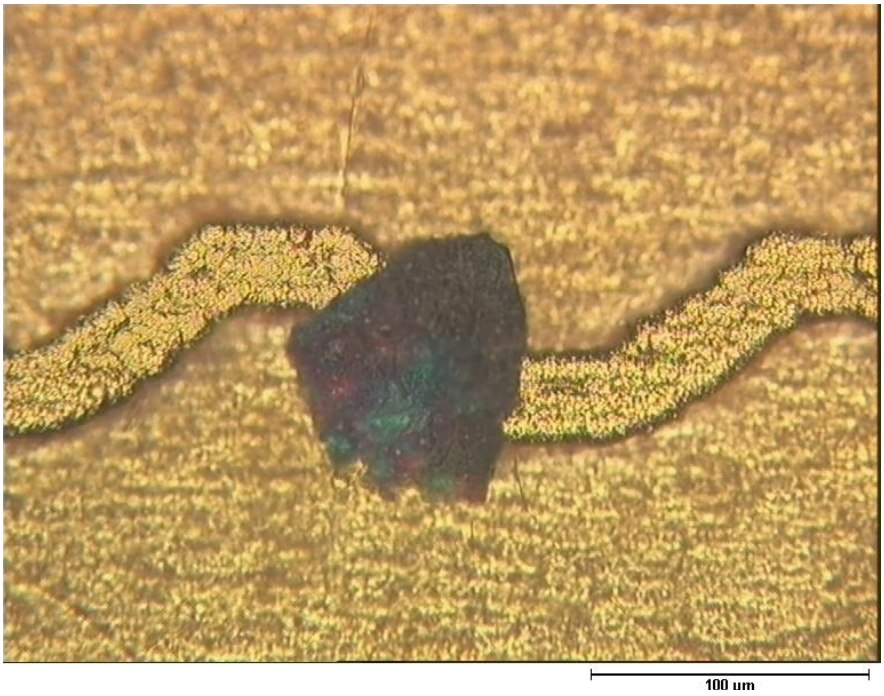


**Figure 3.15: Particle over a gold path -**

allow resist residues to remain and ruin the gold plating (Fig. 3.17).

Reducing the prebaking time to 5 minutes and increasing the energy per surface unit in the LDI allowed us to obtain even better results and to reduce considerably the development time. The best results were obtained by setting an energy of 900 mJ/cm$^2$ in the LDI and developing for 2:20 minutes in AZ developer diluted 1:1 with distilled water, at room temperature and shaking firmly. With these parameters we could not achieve sharp edges, but rather gradual slopes (Fig. 3.18). This would give to the gold structures a mushroom shaped cross section which could help later to hold the structures inside the polyurethane matrix during the etching of the copper foil.

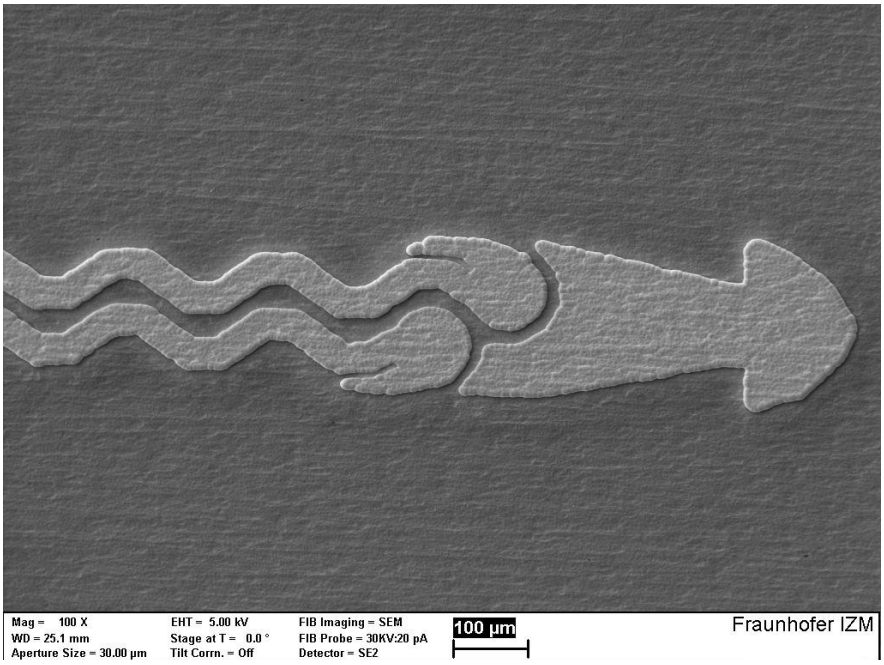


**Figure 3.16: Gold structures wider than designed.** - The first tests with AZ resist resulted in overdeveloped samples, growing the gold structures behind the designed border. The image shows how the distance between paths has been reduced. SEM image.

## 3.4 Electrode gold plating

Gold electroplating for different applications has been extensively tested in the chemistry laboratory at Fraunhofer IZM. This know-how was directly used in the present work with almost no changes.

First pre-tests using KOLON dry resist showed a very strong dependence on the pH value, where under pH 5.5 would show incomplete plating, probably due to the formation of hydrogen bubbles, and over 5.7 would cause some delamination and gold would be plated outside the structured area.

The use of AZ-4562 liquid resist eliminates this problem, because it stands much higher pH values and a fine pH adjustment was not needed any more. We found that leaving the pH untouched after making up the electroplating bath, usually around pH 6.1, would provide good results.

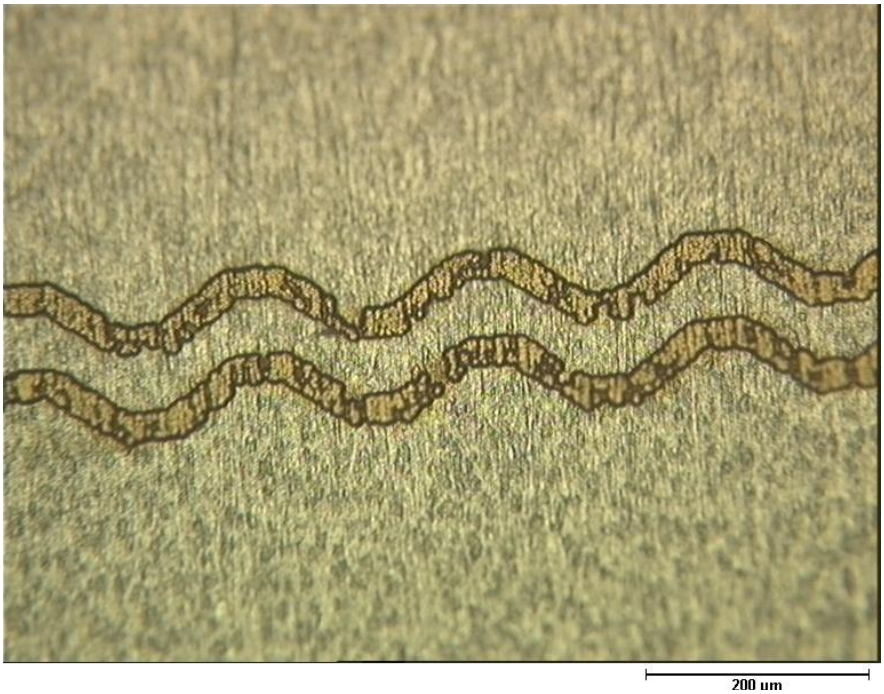


**Figure 3.17: Incomplete gold structures.** - Disturbed gold structures after exposisng AZ resist to 450 mJ/cm$^2$ and developing for 6 minutes in 1:1 diluted AZ developer. The irregularities are caused by resist residues in the exposed areas. Optic microscopy image.

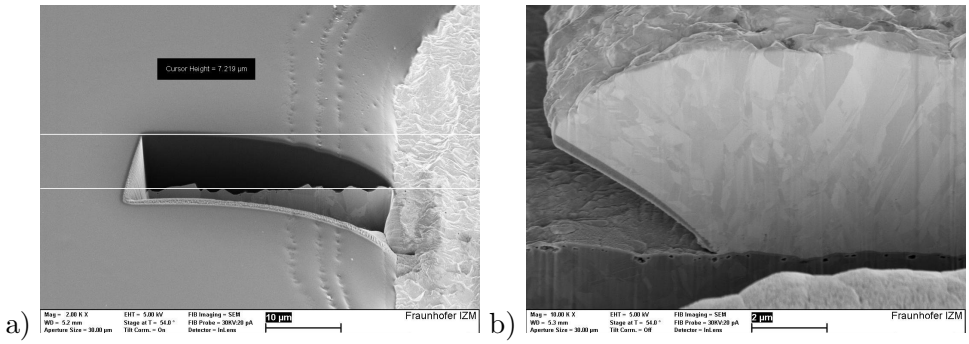


**Figure 3.18: Gradual slopes at photoresist edge.** - Right after development (a) and after gold plating and removing the resist (b). The slope is transfered to the gold structures, giving them a wedge like shape that will be useful in subsequent steps, as it will stabilize the gold in the polyurethane matrix.

## 3.5 Contacts reinforcement

Although not foreseen in the original process proposal 2.1, a second plating process was discovered to be needed after trying to open the polyurethane surface with a laser beam in order to open a blind via that reaches the gold structure, where the contact with the nerve is to be built (see 3.9). The laser used could not be controlled with enough precision in order to guarantee a good result, and most of the gold under the hole in the PU would melt, causing delamination and burning the underlying PU (Fig. 3.19).

a) 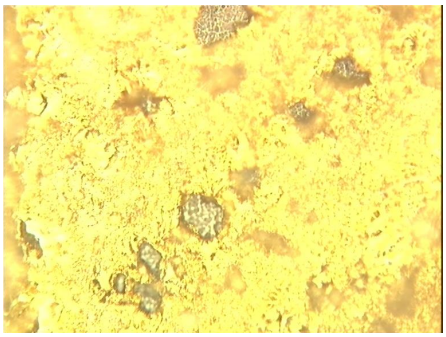 b) 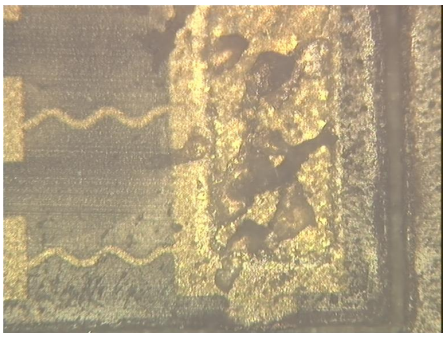

**Figure 3.19: Damaged gold after opening a blind via** - Gold layer embedded in PU damaged after removing the PU with laser.

The solution found was plating a thick (around 20 $\mu$m) layer of gold over the already plated structures (which usually are between 5 and 10 $\mu$m thick). After encapsulating the gold structures in polyurethane the twice plated areas would be covered by a much thinner layer of PU, reducing the required laser energy, and would offer a much higher heat absorbing capacity. Both characteristics would reduce the temperature the gold would reach outside the areas directly irradiated by the laser beam, thus not damaging the PU-gold interface around the contact areas.

### 3.5.1 AZ 4562 photoresist

In the first plating step AZ 4562 liquid photoresist was found to be the most suitable, but two important problems were expected to arise: first, spinning a sample with already built structures of height similar to the final thickness of the coating (around

10 $\mu$m) could lead to unpredictable results, and second, vertical resist edges would be needed, something we could never achieve with this photoresist.

### 3.5.2 KL 1015 photoresist

The only available dry resist in the beginning was the KL1015, which we had already tested for the first plating step. Nevertheless this resist was far too thin, 15 $\mu$m, for the structures we needed, of over 20 $\mu$m, to get the electrode pad to reach the PU surface (see 3.9). To overcome this problem, we tried laminating twice the samples. We started with the standard parameters for both laminations, setting the laminator rolls to 110°C and trying speeds between 0.3 and 0.5 m/min. But some air bubbles would always appear behind the gold structures, at the edges perpendicular to the movement. After trying different parameters, we found that by introducing the sample tilted to the laminator (some 45°), 120°C and 0.1 m/min for the first lamination and 90°C and 0.3 m/min for the second one, the bubble formation could be avoided. As expected, we could not avoid some light delamination near the plated areas, resulting in a halo like gold plating patern around them (Fig. 3.20 a and b). After 30 seconds submerged in GoldStripper 645 this thin layer could not be seen anymore (Fig. 3.20 c and d). This last step originated however some problems further in the process (see 3.7), and had to be removed.

### 3.5.3 RD 1225 photoresist

We started then testing a dry photoresist recently purchased by the group and which optimal working parameters had not been extensively tested, the RD 1225 manufactured by Hitachi Chemicals.

To look for good parameters we used a test design containing lines and dots of different sizes, from 200 $\mu$m diameter or width down to 20 $\mu$m. The resist was laminated in three silver plated copper foil samples, exposed in the LDI and developed in the in-line developer 20 minutes after exposure, using the recommended parameters. The only varied parameter was the exposure energy (25, 30 and 35 mJ/cm$^2$), within the recommended values. With 25 mJ/cm$^2$ the resist was not stable enough and was damaged by the rollers inside the developer. 30 mJ/cm$^2$ seemed to be sufficient for

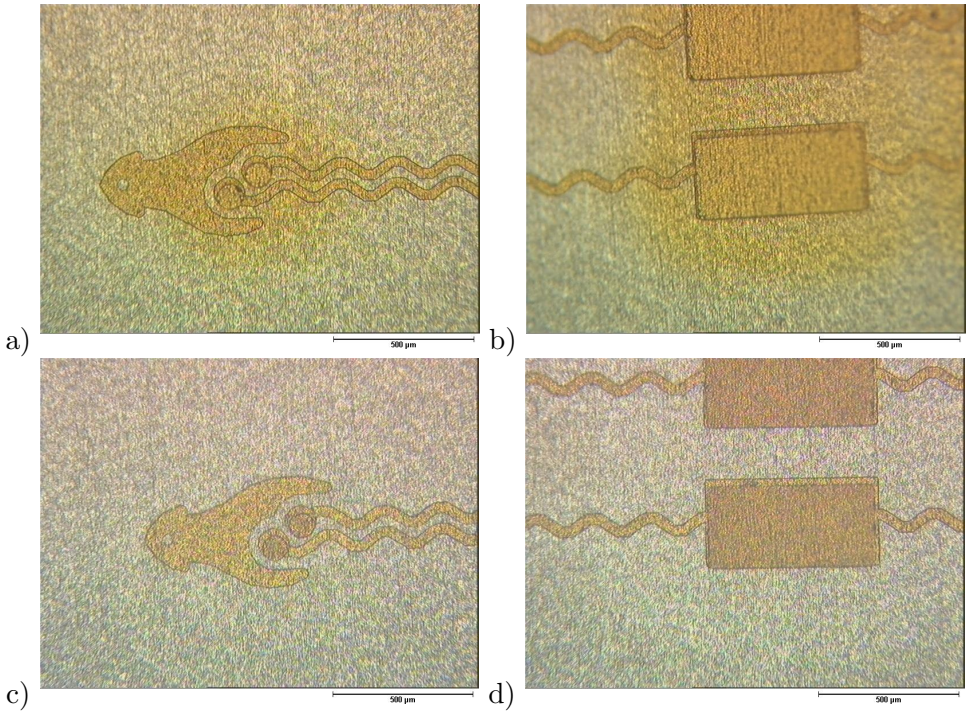


**Figure 3.20: Removal of gold halo** - After stripping the KL1015 resist. A halo-like thin gold layer can be observed around the plated areas (a and b). The same samples after 30 seconds in Gold Stripper at room temperature. The gold halo has completely disappeared (c and d).

the resists stability and the 30 $\mu$m diameter dots had been clearly opened. With 35 mJ/cm$^2$ only the dots from 40 $\mu$m on were opened. We observed that developing the samples twice, or doubling the developing time would allow also the 25 $\mu$m dots to be successfully developed. Another effect was that the final diameter of the holes was around 5 $\mu$m less than the original designed diameter (see 6.1.4), what would allow us to produce cylindrical contacts with a minimum diameter of 20 $\mu$m.

A further step had to be added because when trying to achieve the smallest contacts possible (around 20 $\mu$m) we observed than less than half of them would be plated (Fig. 3.21), probably due to the presence of an air bubble inside the hole in the resist, an effect that could be expected, as the height-diameter ratio is near to or even bigger than 1.

This problem was solved using a plasma superficial treatment. Oxygen and argon were tried, with similar results, but argon is preferred to avoid the severe oxidation caused by oxygen plasma in the case where some silver surface remained uncoated.

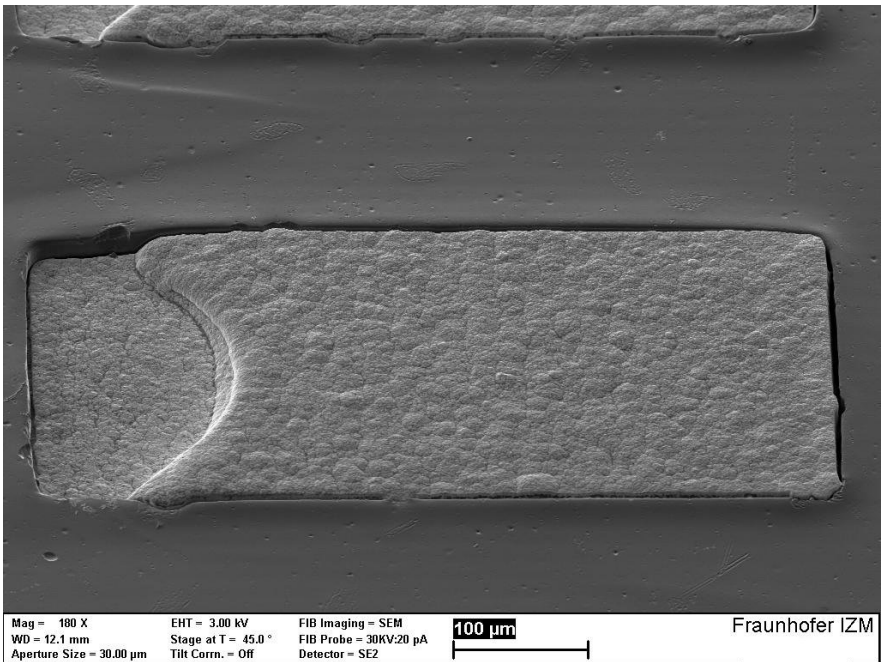


**Figure 3.21: Disturbed gold plating** - Gold pad partially not plated, probably due to the presence of an air or hydrogen bubble during the plating process. SEM image.

## 3.6 Polyurethane embedding

### 3.6.1 Introduction

The optimal parameters for encapsulation of Cu circuits in TPU had already been researched within the framework of the EU project STELLA and, though the requirements were not exactly equivalent, were directly tried on the E-Nerv samples. The samples will be laminated twice with a 25 $\mu$m thick TPU sheet. The first lamination, prior to the copper etching process, requires the TPU to completely melt in order to fill the cavities between the silver surface and the gold structures and to solidify around the electrode contacts avoiding the appearance of internal stresses in the PU. Trails in this TPU layer suggest that it flows for several millimeters before it solidifies (Fig. 3.22). The second lamination, once the copper base has been removed, completely encloses the gold structures in a TPU matrix. As the only physical support of the gold structures during this lamination process is the first TPU layer, the temperature has to be low enough to prevent this PU layer from flowing, as it would drag the structures in an unpredictable way, making the sample useless. But the temperature has to be high enough to permit both layers to glue together in a very stable way.

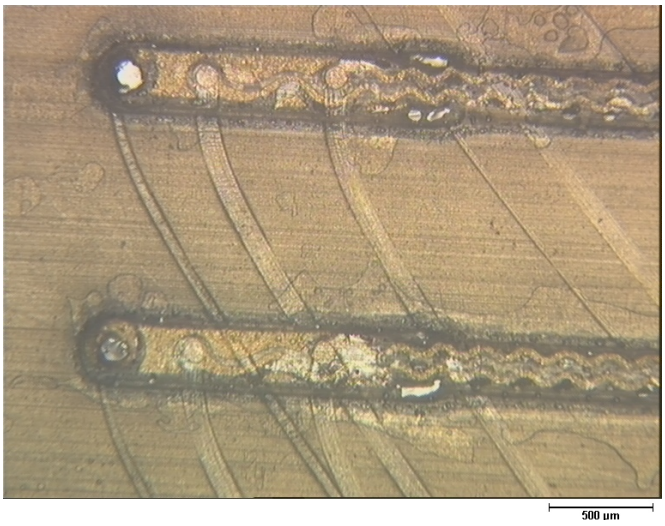


**Figure 3.22: Trails in the PU layer** - Originated in the reinforced contacts, suggesting that the PU flows for, at least, several milimeters during the lamination process. Optic microscopy image.

### 3.6.2 First lamination

The process used for copper structures turned out to behave properly for our purpose, and the pressing parameters were not changed. As rigid support, a 1 mm epoxy board was used. Its surface is quite uneven, and therefore we placed a 200 $\mu$m TPU sheet over it, covered with a PTFE-impregnated stiffener. The 25 $\mu$m TPU sheet was placed over the stiffener and then the sample, with the gold structure in contact with the TPU. The stiffener turned out to have an undulated surface with some holes where the glass fibers intersect, resulting, when covered with the PU layer, in a non planar PU surface with towers reaching almost 100 $\mu$m high (Fig. 3.23). This problem was avoided by insetting a 25 $\mu$m PTFE layer between the stiffener and the 25 $\mu$m TPU.

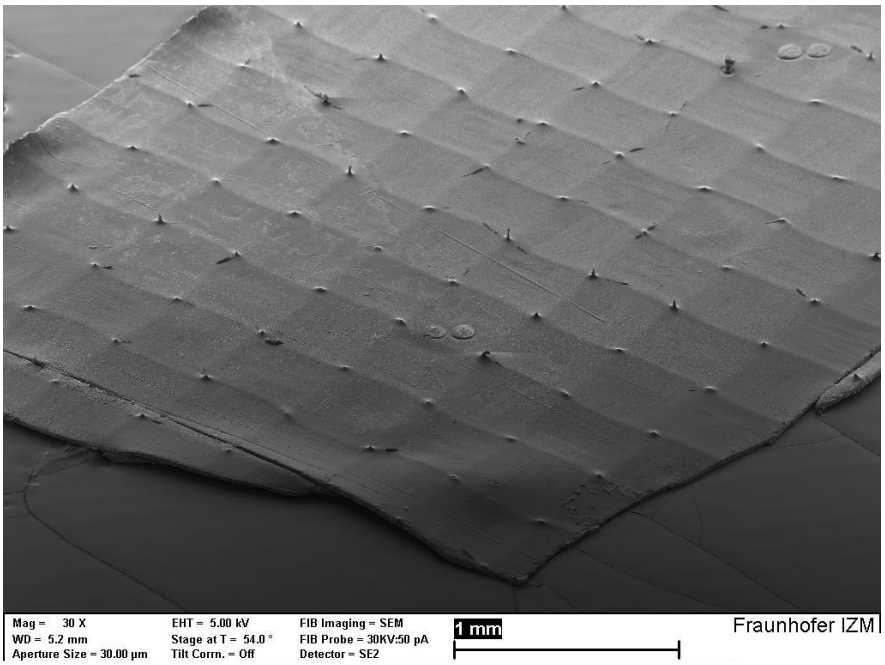


**Figure 3.23: Pikes on the PU surface** - Caused by holes in the stiffener layer. SEM image.

### 3.6.3 Second lamination

The gold structures in the E-Nerv project are of a much smaller scale than those of copper for which the original lamination process was designed. As result, the tips of the gold conducting paths tend to move, dragged by the softened TPU for distances

no bigger than 50 $\mu$m, what would render the electrodes useless, as in many cases it established contact between them. The figures in 3.24 show how the electrodes have changed their relative position in different ways, being dragged by the softened TPU while it flows outwards. This effect is very sensitive to the maximal temperature of the process. The electrodes shown in 3.24 were pressed with a maximal temperature of 165°C. Cutting down this value to 160°C reduced the relative movements within the electrodes tip to less than 5 $\mu$m, an acceptable value.

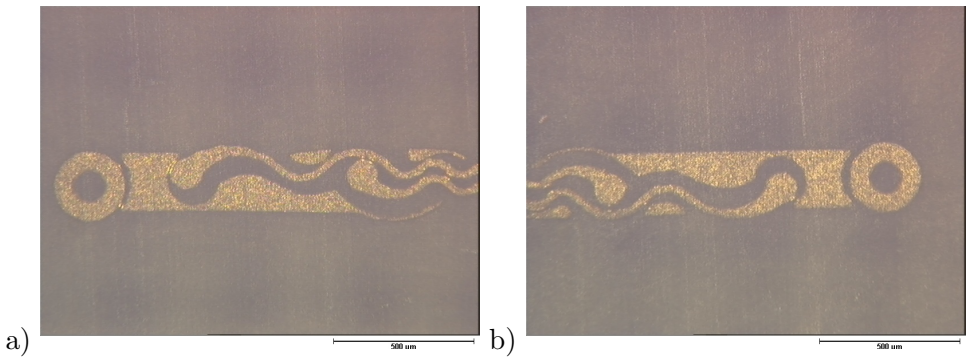


**Figure 3.24: Deformed electrodes** - The PU matrix has become fluid during the second lamination, dragging the electrode towards the sample's borders. (a) is in the top half of the sample and (b) in the bottom half. Optic microscopy image.

## 3.7 Copper etchig

Once the gold structures have been encapsulated in polyurethane through a lamination process, the silver plated copper foil that serves as base material has to be removed. The method chosen is to chemically etch it with an alkaline copper chloride based etchant(17). The silver is very slowly dissolved in it, but the outer silver layer detaches from the copper surface as the latter dissolves through the pores present in the silver layer, and can be removed with a tissue after 10 minutes of etching. The air bubbles flow over the surface is important, as an irregular flow will cause some areas to etch faster than others. The etching process can take between 30 and 45 minutes until all the copper has been removed.

### 3.7.1 Removal of non-Copper residues

**Silver** After the whole copper sheet has been etched, the silver coating usually remains attached to the polyurethane in the areas that took more time to etch, due probably to irregularities in the air flow. Although these silver rests can be removed by continuing the etching process, we found an alternative that avoided the physical stress caused by the air bubbles and did not require the 50°C of the etchant, consisting of a room temperature 10% nitric acid solution with iron (III) nitrate nonahydrate. Tests have been done with concentrations ranging from 2 to 10 g/l, all with satisfying results.

Even in samples that seemed to be silver-free under dark field optic microscopy resulted to contain some amount of silver rests over the polyurethane surface (Fig. 3.25), easily seen through bright field microscopy. As their effect on the layers conductivity had not been tested, we decided to eliminate them in the iron (III) nitrate nonahydrate solution with 10% nitric acid. After 20 minutes the dark spots had completely disappeared.

**Gold** In some of the samples a grey layer could be seen over the PU after etching the copper. It showed to have conducting properties, what would short-circuit the electrodes. Trying to remove it physically (Fig. 3.26) allowed us to realize that it had some polymer-like characteristics. It seemed like the polyurethane impregnated some conducting particles on the silver surface of the sample, in a concentration high enough

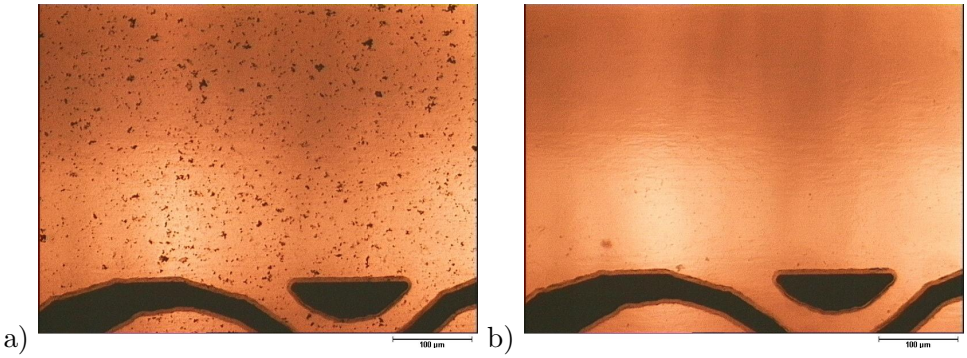


**Figure 3.25: Removal of silver particles embedded in the polyurethane** - Silver crystals remaining in the pits on the PU surface after copper etching (a). Same spot of the sample after 20 minutes in the iron nitrate solution (b). Optic microscopy image.

to become an electric conductor itself. The first supposition was that it could be some silver compound, probably silver oxide. We tried with 10% nitric acid solution with iron (III) nitrate nonahydrate, with hydrochloric acid, with ammonia and reducing it with aluminium in a sodium carbonate solution. Nothing seemed to change. A detailed x-ray spectroscopy test showed the presence of gold nanoparticles 6.1.7. And, indeed, 5 seconds in Gold Stripper 645 completely removed the grey layer. This effect was only found in samples where the second gold plating process involved using the KL-1015 photoresist. It was permeable enough to the gold electrolyte to build some halo-like features around the plated structures. To remove them, essential to avoid a short-circuit, the samples were treated with Gold Stripper 645 right after stripping the resist. The gold nanoparticles could have remained in spite of the gold stripping, or could have been deposited from the gold stripper as part of a exchange reaction with the underlying copper through pores in the silver coating.

After choosing RD-1225 as photoresist for building the contact reinforcements, no more gold stripping was necessary and this problem disappeared.

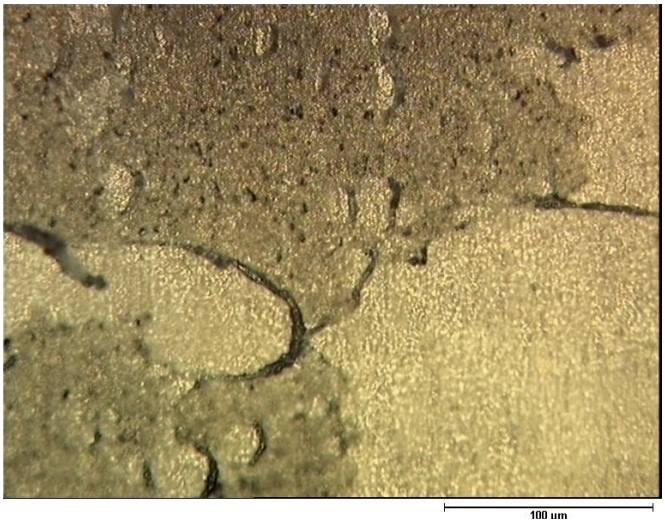


**Figure 3.26: Dark conductive layer on the PU** - Partially removed by rubbing. Optic microscopy image.

## 3.8 Electrode cutting

Once the gold structures are embedded in the polyurethane matrix, the bounds that define the electrode have to be laser cut. This step decides the final length of the electrode tips, eliminating the polyurethane between them. Right behind the contacts of the electrode tip a polyurethane spur has been added aimed to make it more difficult for the contacts to move backwards.

In this step it is very critical to achieve a complete cut along the hole edge of the electrode as, otherwise, the tensions that appear when trying to remove the electrode from the board can easily lead to a mechanical failure in the gold conductive paths, rendering the electrode useless (Fig. 3.27).

To avoid this, we increased the laser energy until also the PTFE foil under it was also totally cut, and focused the beam at the interface between the PU foil and the PTFE. A second advantage of cutting the PTFE foil is that it can be removed from the board along with the electrode, providing better resistance to folding and thus making handling easier.

What could not be avoided was the formation of bubbles inside the PU near the edge

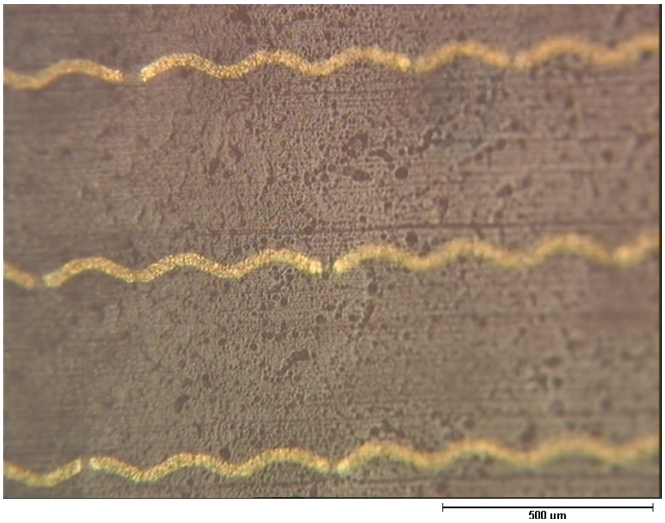


**Figure 3.27: Broken conductive paths embedded in PU** - Due to excessive elongation while removing from board an electrode not properly cut. Optic microscopy image.

of the electrodes (Fig. 3.28), due to the high temperatures reached during the cutting process. This could affect the permeability of the PU cover, thought the conductance measured between lines in physiological solution suggest that it remains within acceptable values. This reason led us to perform some tests aimed to verify the isolation provided by the PU in these conditions (see 6.1.6).

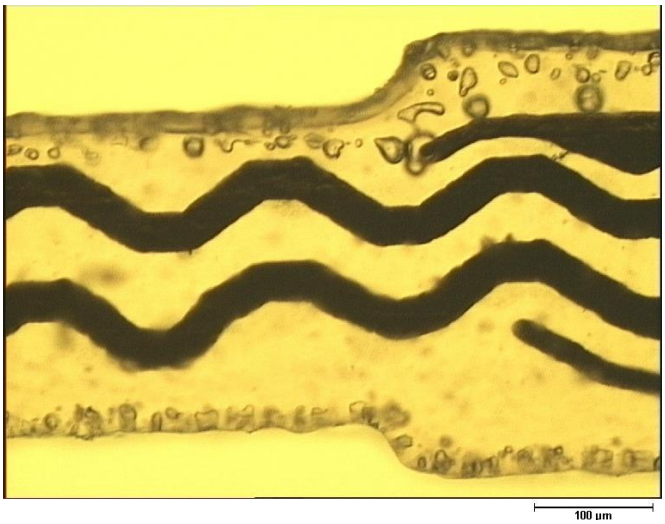


**Figure 3.28: Bubbles in PU near the edge** - Due to the characteristics of the laser used, part of the electrode's PU is heated up and bubbles appear. Optic microscopy image.

## 3.9 Contac drilling

Once the gold structures have been encapsulated in TPU, the electrode contacts have to be somehow opened free to achieve contact with the nerve surface. A pulse laser was to be used for this purpose, evaporating the 25 $\mu$m TPU covering the 7 $\mu$m thick gold contacts. The equipement used was the Siemens-Dematic MricroBeam 3500/3205 pulsed laser driller. 1.5.1

The first experiments showed that the energy required to remove the 25 $\mu$m of TPU and allow the gold beneath to remain undamaged was in a very narrow window, what meant that using the same parameters for neighbour electrodes resulted in an important amount of remaining TPU (Fig. 3.29 a) in some cases or also in the gold being drilled through in other cases (Fig. 3.29 b).

a) 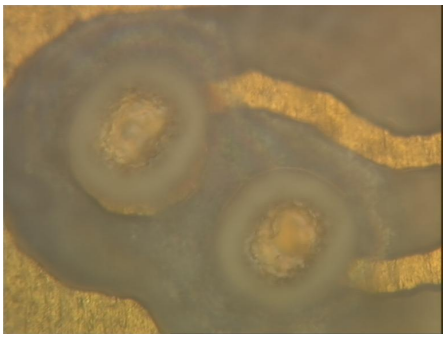 b) 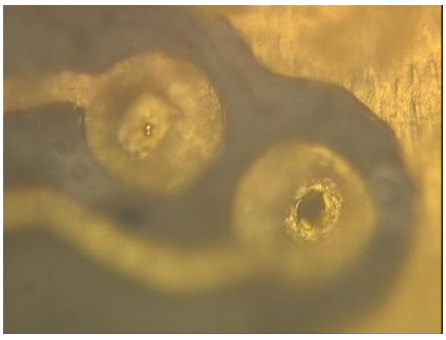

**Figure 3.29: Different bad drilling results with same parameters** - Some PU remains over the gold pads after laser drilling (a). The PU over the pads has been removed, but also the gold has been damaged (b). Optic microscopy image.

In order to face this problem, we decided to reinforce the electrode contacts with plated gold [See Dry resist and 2nd plating], some extra 20 $\mu$m, what would leave less than one $\mu$m of TPU to be removed. This means that not only the required energy could be lowered, but also that the reinforced gold could accept more energy before reaching enough temperature to affect to the TPU-gold interface stability.

Different drilling parameters were tested until acceptable results could be obtained. 6.1.5

## 3.10 Contact nano-structuring

### 3.10.1 Introduction

A nanostructured electrode contact surface provides a much bigger contact area, what would improve the robustness and output signal intensity, while increasing the adherence of the electrodes to the nerve cells (Ref. (18)).

Researching in the field of solderless contacting, my supervisors, Michael Zwanzig and Ralf Schmidt, found the optimal parameters to build gold nanostructures with a shark teeth-like shape, using a pH controlled gold cyanide electrolyte.

These structures have a similar scale to the regular column structures researched by Craighead et al. (Ref. (18)), between 500 nm and 5 $\mu$m. The cells tend to prefer the structured areas and attach to the top of the columns.

Therefore we decided to fill the gold contacts with "shark teeth"nano-structured gold.

### 3.10.2 Development

For the first tests we used a 7 $cm^2$ sacrificial platinum cathode. We set the optimal parameters to obtain the shark teeth structures previously found by M. Zwanzig and R. Schmidt and electroplated an electrode for 10 minutes. All the 6 treated electrode contacts did galvanize, what confirmed that the gold electric paths were at least conducting. But the result (Figs. 3.30) showed that far too much gold was plated, and its surface was covered with unexpected structures: terraced pyramids, with a five-pointed star base and height from 500 nm to 3 $\mu$m, similar to those found one some silver electroplated surfaces. For some reason, the current flowing through the contacts was much bigger than calculated. We had supposed that the current density would be the same in the E-Nerv electrode contacts and in the thief.

Electroplating another electrode for 1 minute did not provide any shark-teeth structures (Figs. 3.31).

Two hypotheses were developed: either being the electrolyte a used one, some

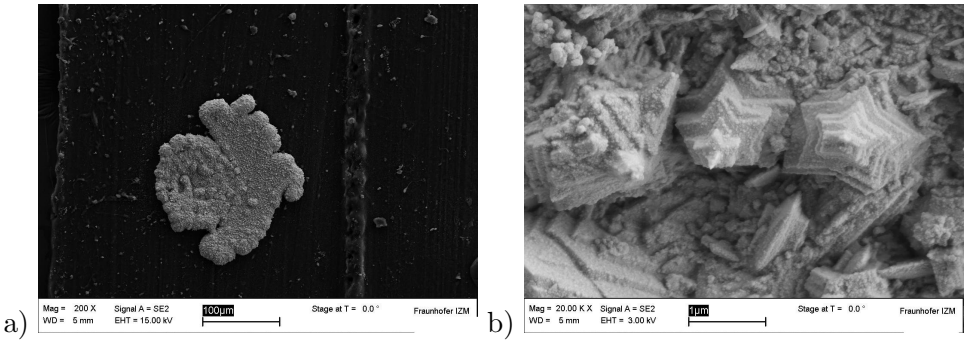


**Figure 3.30: Overplated contacts despite using previously tested parameters** - Overplated contact after 10 minutes electroplating with thief (a). Unexpected star-shaped gold crystals (b). SEM images.

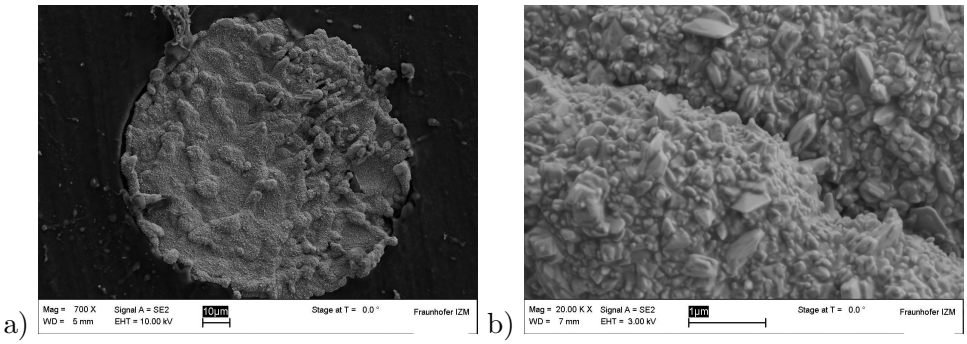


**Figure 3.31: Plated contacts where shark-teeth didn't form** - 1 minute electroplating with sacrificual cathode (a). Surface does not show the expected shark-teeth structures (b). SEM images.

silver contamination could have forced the gold to crystallize in a silver-like pattern, or the current did not distribute equally between the electrode and the thief, because the contact methods for both were different and could present very different electrical resistance.

In order to understand the trend of the relationship between size of a pad and distribution of current density, we performed a test where pads of different sizes were connected to the same current source. The results obtained are showed in graph 3.32.

This explained the strong overplating observed when using a thief, and led us to think that small surfaces like our electrode (under 0.01 $mm^2$ per contact) could require

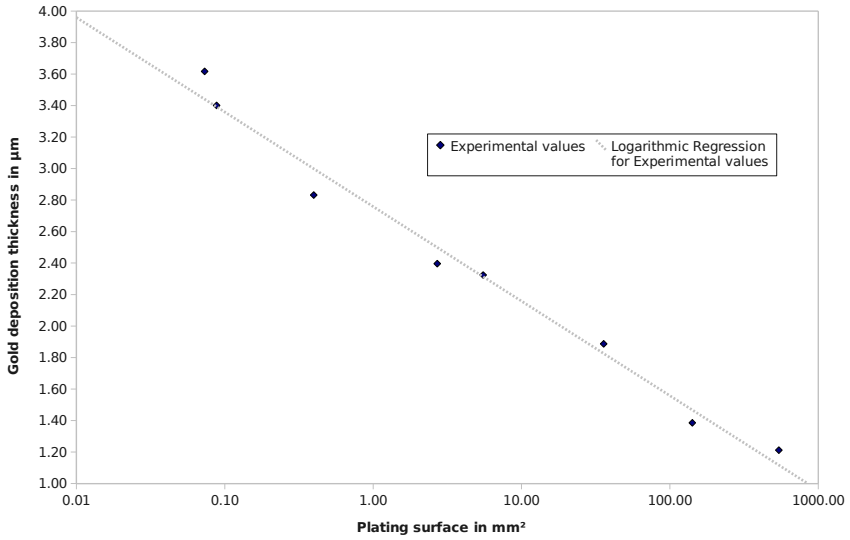


**Figure 3.32: Graph showing effects of area size on current density** - Horizontal axis is in logarithmic scale.

higher current densities to obtain proper shark-teeth structures.

A new electrolyte was made up and, as the specifications of the current source employed (SourceMeter®Model 2400 from Keithley Instruments, Inc.) indicated that the device can accurately provide the required current of around 1.2 $\mu$A, the thief was discarded. The result, after 10 minutes plating, would not offer any difference from the unplated gold surface. Plating an electrode under the same conditions with Puramet 202 electrolyte showed that at least some deposition took place (Fig. 3.33), what meant that the current was actually flowing through the electrodes surface. This confirmed that the calculated current was not the optimal for building shark-teeth structures under these conditions, as the value had been extrapolated from gold pads in PCB with other shape, disposition, size and isolating material.

As using a thief had brought some results, although not optimal, we measured the current flowing through the electrode when using a thief. The thief has an area of 7 $cm^2$, what requires a total current of 17,5 mA to have the 2,5 $mA/cm^2$ needed. Measuring the current that actually flows trough the electrodes shows that it is between 10 and 20 times higher than the corresponding current to the area of the electrodes. The total

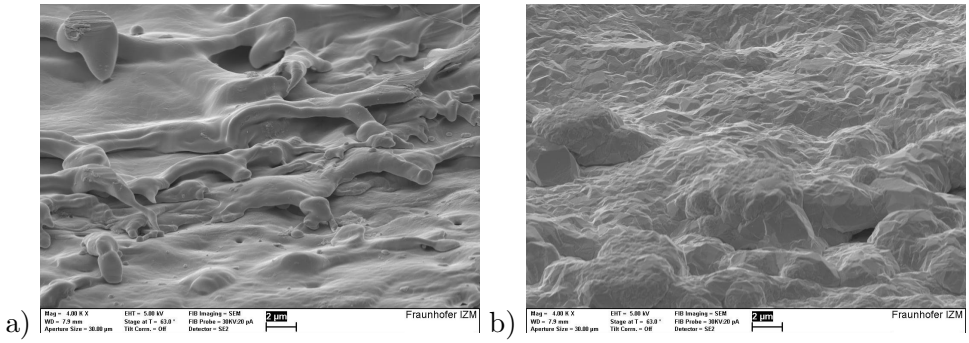


**Figure 3.33: Contacts plated with Puramet 202** - Contact surface after removing the polyurethane with laser pulses (a). Contact surface after plating with Puramet 202 without using a thief (b). SEM images.

current had to be set to under 1 mA to obtain the 1,2 $\mu$A required in the electrodes. Next we plated an electrode setting the total current to 5 mA, obtaining the following current values through the electrode in 10 minutes: (see graph. 3.34).

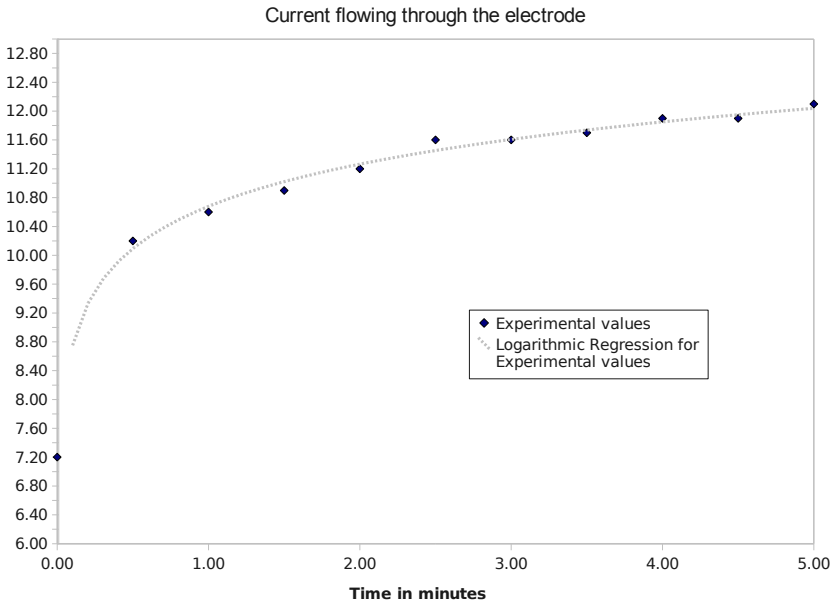


**Figure 3.34: Graph showing the evolution of the current taken by the electrode** - The current absorbed increases as the deposition takes place.

The current absorbed increases as the deposition takes place, and even since the

beginning, it is much higher than the 1.2 $\mu$A predicted. The SEM pictures show how huge gold crystals were build on the outer circle of the electrodes (Fig. 3.35), while the centre showed something more similar to the expected shark-teeth structures, but with the areas between these structures filled with smaller crystals.

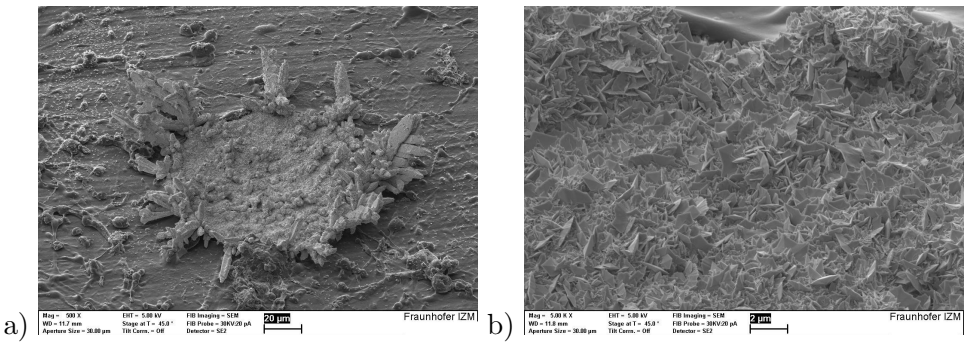


**Figure 3.35: Huge crystals around the contact** - Huge gold crystals around the outer circle of the contact after plating for 5 minutes with thief (a). However, the inner area of the contact shows structures much more similar to the expected shark-teeth (b). SEM images.

This characteristics had been previously found by higher than optimal current densities in Ralf Schmidt and Michael Zwanzig previous work. As next step we tried controlling the total provided current aiming to obtain a constant current through the electrode contacts (see graph 3.37). The previous experiments suggested that the optimal current was substantially lower than 10 $\mu$A but higher than the calculated 1.2 $\mu$m. We decided to start with 3 $\mu$A, what would mean around 7 mA/cm$^2$, or more than twice the optimal value found under electroplating test conditions. The result showed a much more homogeneous crystallization pattern (Fig. 3.36), but with features that did not correspond exactly to the expected shark-teeth, with many small and irregular crystals.

After this positive result, we removed the thief and set the total current to 3 $\mu$A. In this case, due to a break in a conducting path, only 5 out of 6 contacts did electroplate, implying a current intensity of 0.6 $\mu$A per contact. The result (Fig. 3.38) was, however, better then the previous one, what made us think that the optimal current was above 3 $\mu$A, and at least nearer to 3.6 $\mu$A.

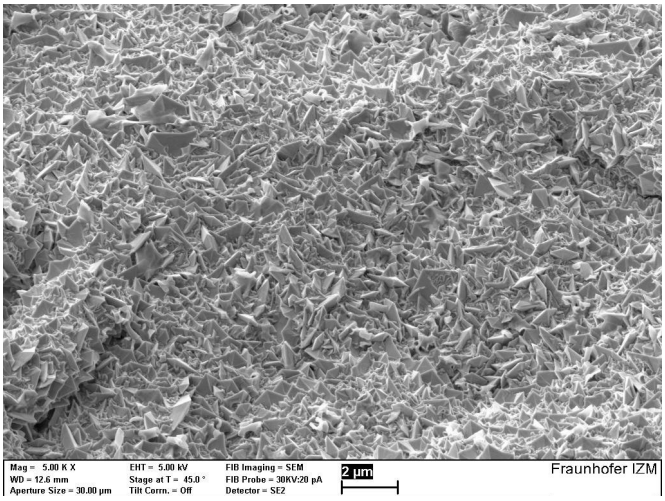


**Figure 3.36: Contact with too small shark-teeth structures** - Contact surface after 10 minutes electroplating with 0.5 $\mu$A per contact. SEM image.

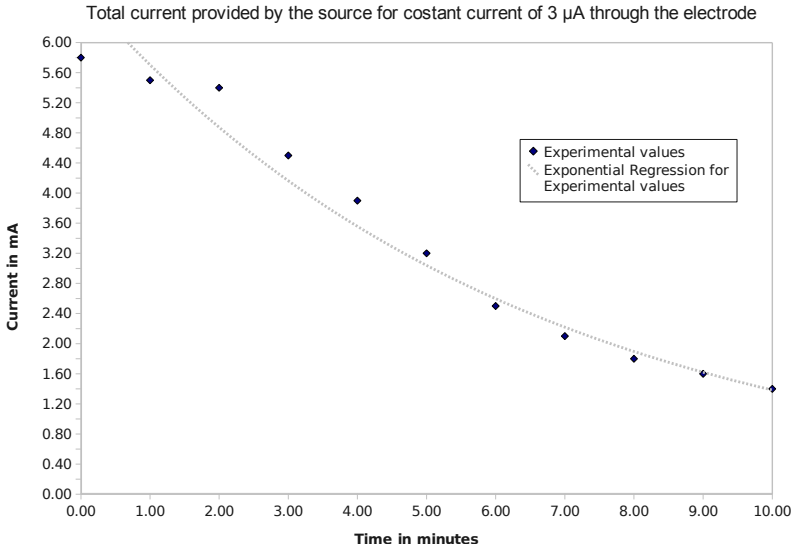


**Figure 3.37: Graph showing the evolution of the current provided by the source** - The current required to maintain constant the current through the electrode diminishes with time.

Working with 3.6 $\mu$A, one of the samples resulted to have two paths broken, what led to a current of 0.9 $\mu$A flowing through each one of the 4 remaining contacts. The resulting surface looked even more similar to the structures we were looking for (Fig. 3.39).

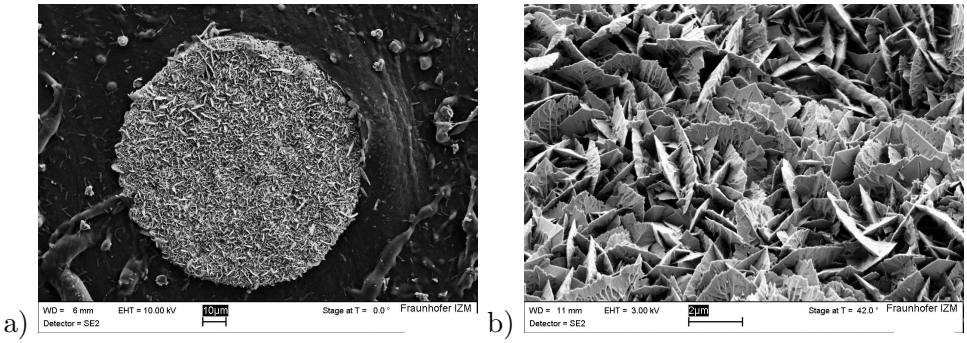


**Figure 3.38: Shark-teeth structures without thief and 3 $\mu$A** - Shark-teeth structures after 10 minutes plating with 0.6 $\mu$A per contact. . SEM images.

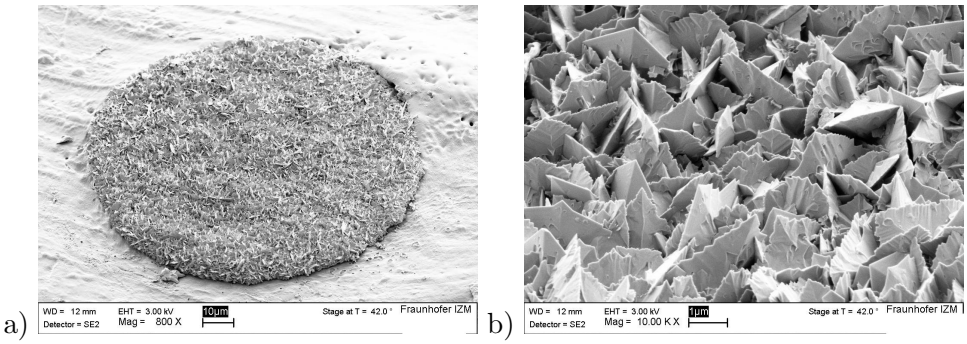


**Figure 3.39: First proper shark-teeth structures** - Proper shark-teeth structures after 10 minutes plating with 0.9 $\mu$A per contact. SEM images.

## 3.11 Electrode contacting

The first in vivo tests of the electrode would require performing at least two and probably three measurements separated several months from each other. A special connector has to be designed to contact the electrodes and transfer the signals to the measuring device, as contacting simply with needles was reported to be very problematic, because the distance between pads is of just 200 $\mu$m.

Due to time and budget limitations, we had to design and build a suitable contacting clamp using only the in house available technology.

We first decided to use needles with 100 $\mu$m in diameter inserted in a PCB piece (see 6.9) that diverts the signals to bigger contact pads where soldering a wire is easier. A PMMA holder (see 6.8) was also designed and milled in order to be able to place

the electrode and the PCB piece correctly (Fig. 3.40). The needle had to pierce the remaining PU over the reinforced back pad of the electrode, and also pierce partially or totally the pad itself. The fact that this rendered a pad part useless for further measurements together with observed irregularities in the needle topography in the first 500 $\mu$m from the tip and handling problems, made us rejecting this option.

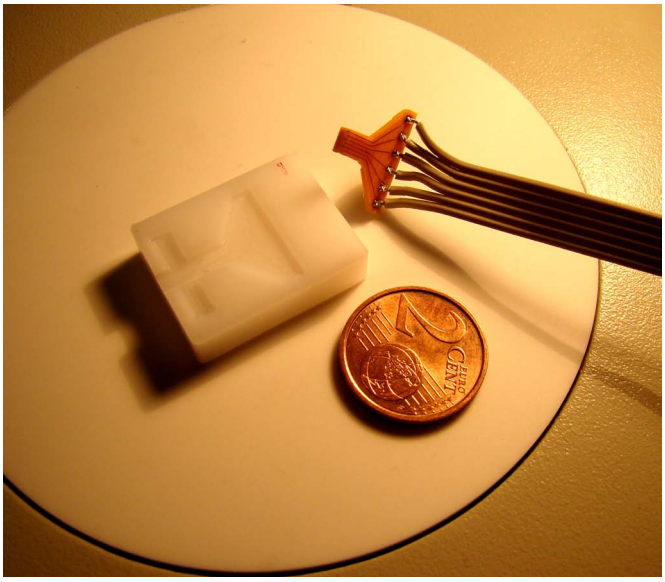


**Figure 3.40: Electrode contacting clamp, consisting of two pieces** - A white PMMA support and a PCB piece where the contacts are built.

As alternative, galvanic copper bumps were grown in substitution of the needle tip, with 50 $\mu$m in diameter and around 15 $\mu$m high. For this reason, the design of the PCB where the pieces were to be built built had to include a circuit for the electroplating current (Fig. 3.42).

To improve surface stability and biocompatibility, the contacts were afterwards coated with nickel and gold. The up to 3 $\mu$m of PU covering the electrode back pads were removed by the same laser procedure used to free the contacts at the tip of the electrode. First tests suggested a contact resistance between 0.2 and 0.3 Ohm, one order of magnitude below the tests performed with needles.

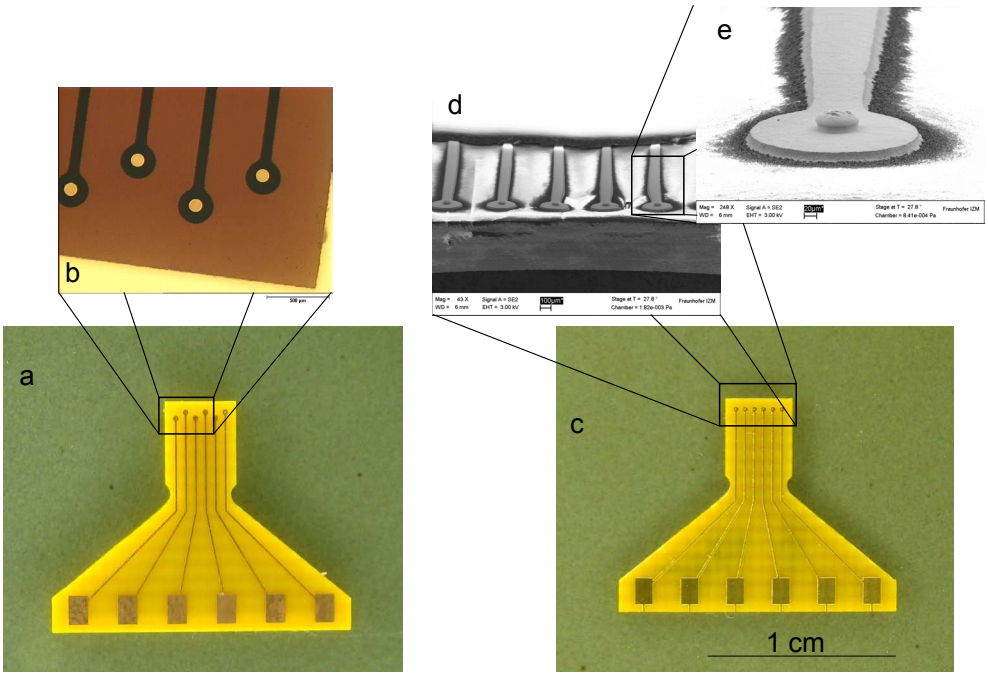


**Figure 3.41: Two approaches for contacting the electrodes** - Using needles tips as external contact surface would require a piece (a) with holes (b) where the needles could be attached. Building bumps on the contact spot (d and e) eliminate the need of a complex needle adjustment, but the hole copper surface has to be plated with gold (c).

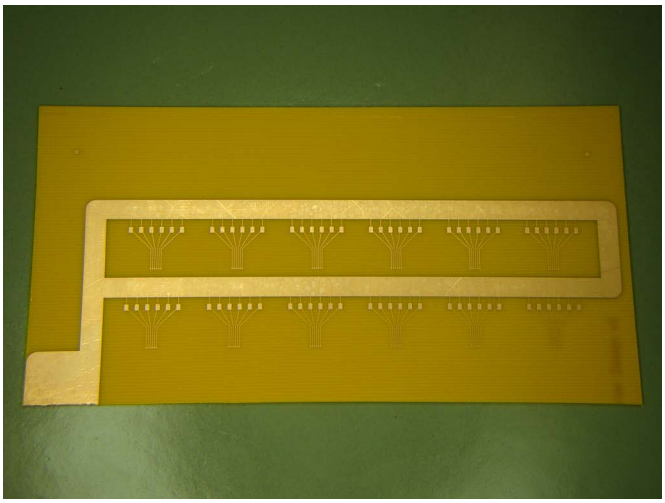

**Figure 3.42: PCB with the contacting clamp design** - Before the Ni and Au electroless baths.

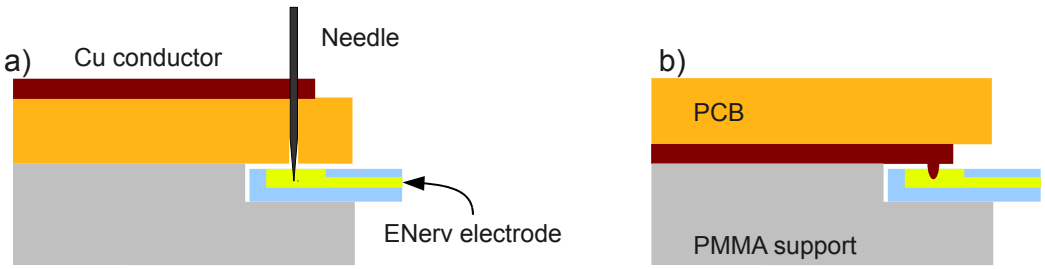


**Figure 3.43: Two approaches for contacting the electrodes** - Needle approach (a) and bump approach (b).

# 4

# Final process

This chapter summarizes the most relevant result of the work, being it the recipe that allows to build functional stretchable electrodes with the characteristics required in the project proposal. Some details, such as the exact composition of the nano-structuring electrolyte, are not explained, because they were not developed within this work and are intellectual property of Fraunhofer IZM.

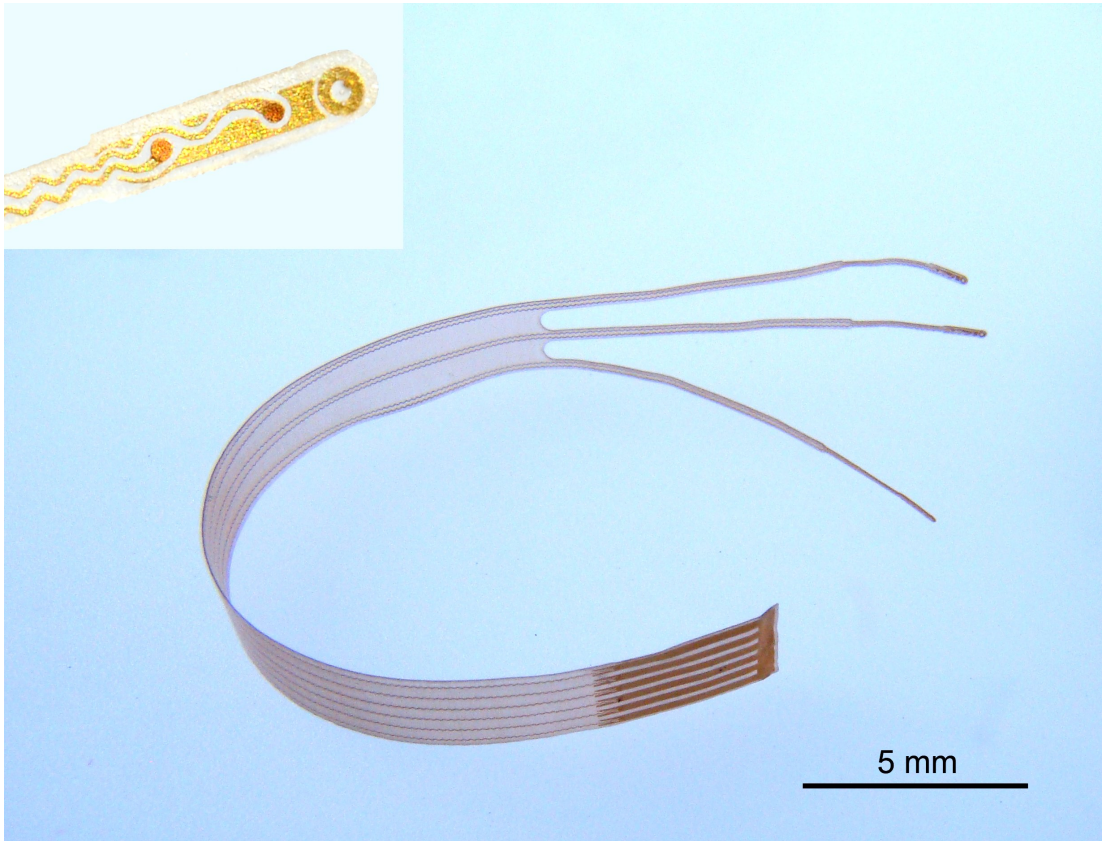


**Figure 4.1: Photograph of a finished electrode** - At the top-left corner, detail of the electrode tip.

## 4.1 Process diagram

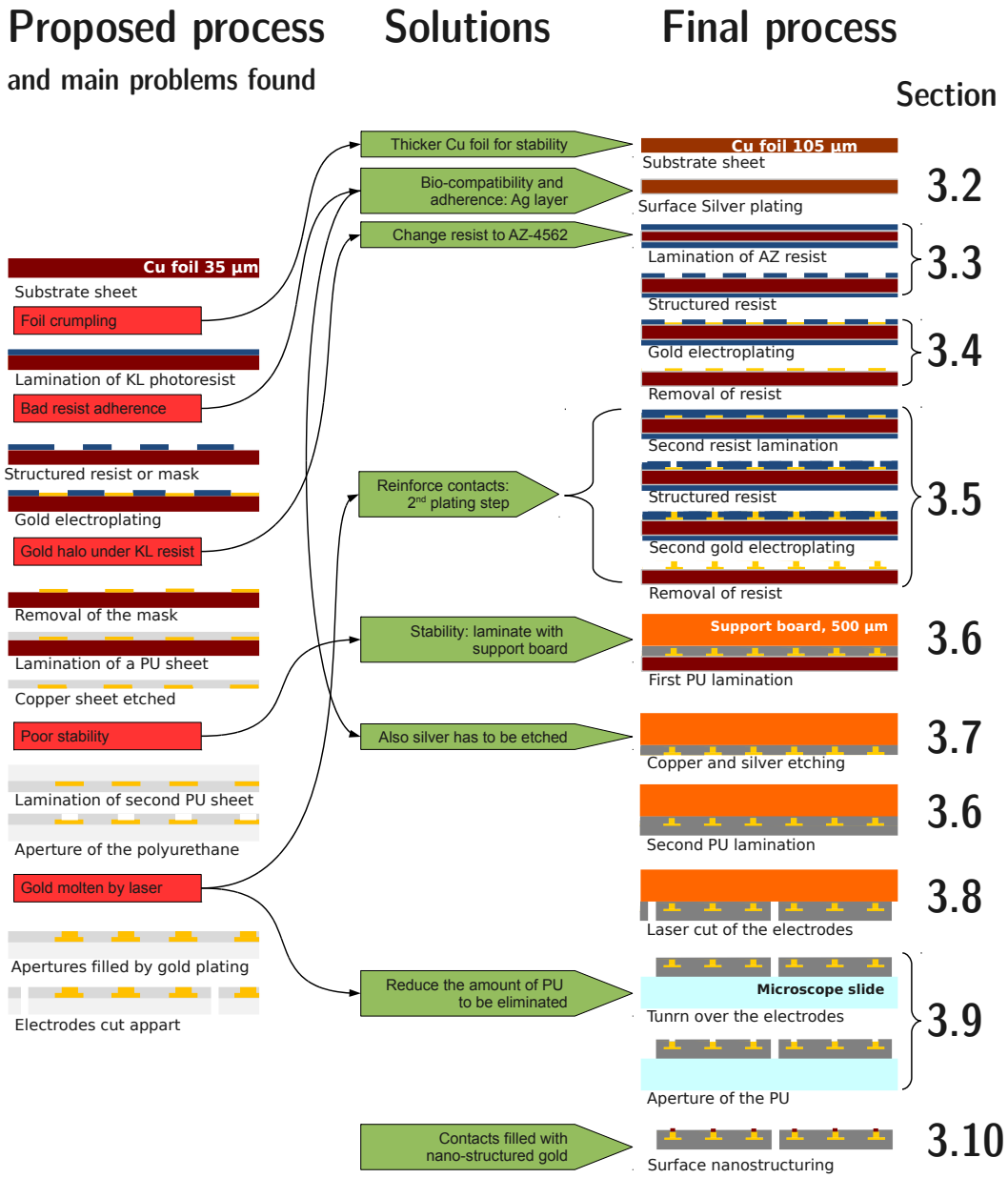


**Figure 4.2: Diagram of the results obtained** - On the left, diagram of the original process proposed when the project started. On the right, final process enabling to produce functional electrodes.

## 4.2 Electrode layout

The final electrode design can be seen in the previous section, fig. 3.4.

## 4.3 Immersion Silver

- Cut a 14x14 cm square from a 105 $\mu$m thick copper foil with one of its sides brushed.
- Drill a hole near to one side, in order to hold it with a stainless steel wire. This way we prevent the sample from having contact with a handler, what could retain some liquid and subsequently contaminate the sample.
- Dip for 3 minutes in Acid Cleaner at 50 °C, with ultrasonic vibrations in 'degas' mode to eliminate particles from the surface.
- Wash with di water.
- Dip for 1:30 minutes in Silver Microetch at 35 °C.
- Wash with di water.
- AlphaSTAR predip for 30 seconds at 40 °C.
- AlphaSTAR silver immersion for 3 minutes at 50 °C, waving gently.
- Wash with di water and dry immediately with nitrogen.
- Store in a bag with protective atmosphere (nitrogen).

The whole process must be performed very carefully, as any drop over the copper surface can originate an oxidation stain that prevents a proper silver deposition on the area.

## 4.4 Electrode structuring

- Make sure the 5 inch vacuum chuck is set in the spinner.
- Use a 15x15 cm (or a bit bigger) board as rigid support.

- Fix the sample with some tape to the board, copper glossy side downwards.
- Place it on the chuck, switch the vacuum on and start the AZ4562 program.
- Close the cover and pour some 3 ml AZ resist over the sample to cover the backside.
- Extract from the machine and carefully remove the tape.
- Place the sample on a tissue on a hotplate at 100°C, coated side upwards, for 5 minutes.
- Clean the board by spinning it with acetone.
- Fix again the sample to the board, this time the glossy side upwards.
- Close the cover and spin the sample with the AZ process pouring acetone for some 20 seconds, when the speed is maximal.
- Run again the AZ process and pour some 3 ml AZ4562 over the sample. Maintain the aperture in the center of the cover closed, to reduce turbulences.
- Remove the tape and place the sample on a tissue on the hotplate, glossy side upwards, for 5 minutes.
- Put the samples in a black bag, separated by clean room tissues.

- In the LDI, import the 001 design with positive polarity and set laser energy density to 900 mJ/cm$^2$ and expose the glossy side.
- Leave the backside unexposed.
- Develop the sample in 1:1 AZ Developer-di water solution by waving it firmly at room temperature for 2:20 minutes.
- Wash with di water for at least 30 seconds, and better in cascade.
- Let the sample dry or dry it with nitrogen.
- Hardbake the sample for 30 minutes at 130°C.

## 4.5 Electrode gold plating

- Make up 0.7 l of Puramet 202 galvanic bath or add the right quantity of gold salt and Puramet 202 organic solution to an already used bath.
- Filter the electrolyte with a Venturi filter using a filter paper for particles smaller than 1 $\mu$m.
- Pour the electrolyte in the preparation box with a magnetic follower and set to 50°C on a hotplate/stirrer.
- Cut the sample and cover its borders with tape (1cm wide galvanic tape). (Fig. 4.3)

a)  b) 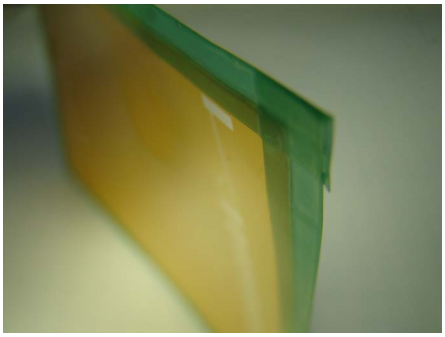

**Figure 4.3: Cut sample and cover borders with green tape** - Cut the sample following the lines in the design (a) and cover the borders with green tape as shown in (b).

- No air bubbles can remain under the tape, as they could be afterwards filled with cyanide containing electrolyte.
- When the bath is ready, dip the sample for 1 minute in room temperature Acid Cleaner, inside an ultrasonic vibration device.
- Wash the sample and dip it immediately in the plating bath (to avoid oxidation) with a 10% of the required plating current.
- Set the full current and plate for 45 minutes, always stirring with the magnetic follower.

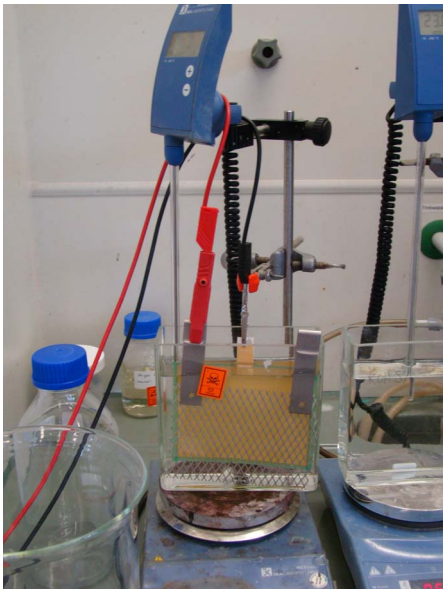

**Figure 4.4: Assembly for the plating step** - Applies to both plating steps

- Stop the current and take the sample out from the bath.
- Wash it and remove the tape (it will probably contain cyanide residues, so discard properly).
- Strip the photoresist in 5% KOH solution at 50°C, stirring fast with a magnetic follower.
- Once the resist is completely dissolved (around 5 minutes), dip in a fresh 5% KOH solution at 50°C, also stirring, for at least 10 minutes, to remove any resist residue.
- Wash thoroughly with di water and dry immediately with nitrogen.
- Store in a bag with nitrogen and sample covered with a clean room tissue.

## 4.6 Contacts reinforcement

- Laminate the samples with RD1225 dry resist, setting the rolls to 120°C and the lamination speed to 0,3 m/min. It is better to give the samples tilted to the rolls,

in order to decrease the probability of having bubbles trapped near the gold edges perpendicular to the laminator rolls.

- Cut out the samples from the resist sheet with an scalpel and let them settle down for 15 minutes.
- In the LDI, load the 002 design.
- Set the panel thickness to 0.16 mm and the laser energy density to 30 mJ/cm$^2$.
- The fiducial registration has to be activated.
- The registration flash time may have to be changed to around 1.3 seconds.
- After the exposure, let the samples settle for 20 minutes before development.
- Develop using the standard developing process for RD1225.

## 4.7 Polyurethane embedding

First lamination:

- Cut a 15x15 cm FR-4 sheet, 0.5 mm thick. Without copper laminated.
- Cut 10x12 cm rectangles of release film ACC-3 (1.5.2) and stiffener ACC-14 (1.5.2) sheets.
- Cut a approximately 20x20 cm sheet of Walopur PU (1.5.2).
- Cover one tray of the Lauffer press (1.5.1) with ACC-3 release film.
- Place the FR-4 square on the film, with a 200 to 250 $\mu$m thick PU sheet over it.
- Place first the ACC-14 and then the ACC-3 rectangles on the middle of the FR-4.
- Cover it with the 25 $\mu$m PU.
- Place the E-Nerv sample over it, with the gold structures downwards.
- Cover again the whole tray with a big ACC-3 film.

- Place two distribution layers over the tray (rubber protected with two ACC-14 and steel sheet).
- Run the standard process for laminating PU.

Second lamination, after Cu etching:

- Cut a approximately 20x20 cm sheet of Walopur PU (1.5.2).
- Cover one tray of the Lauffer press (1.5.1) with ACC-3 release film.
- Place on the tray the etched sample attached to the FR-4. Gold structures upwards.
- Place the PU sheet over the sample.
- Cover again the whole tray with a big ACC-3 film.
- Place two distribution layers over the tray (rubber protected with two ACC-14 and steel sheet).
- Run the following process for laminating PU:

**Table 4.1:** Second PU lamination process

| Time, minutes | 0 | 15 | 25 | 45 | 75 |
|---|---|---|---|---|---|
| Temperature, °C | 50 | 120 | 150 | 160 | 50 |
| Pressure, N/cm$^2$ | 0 | 0 | 0 | 50 | 0 |

## 4.8 Copper etchig

- Attach a stainless steel wire to the sample. An easy way is not to remove all the polyurethane remaining outside the bounds of the sample after the lamination, and inserting the wire through it.
- Heat the etching solution to 50°C and adjust pH, when needed, adding ammonia to reach a value between 8.3 and 8.5.
- Open the air flow and dip the sample for some 10 minutes.

- Take the sample out and clean the remaining silver with a clean room tissue.
- If some areas seem not to be affected by the etching solution, sand them down with fine sandpaper until only clean metallic copper can be seen.
- Dip again in the etching solution, always with air flow, and etch until all the copper has been removed (between 25 and 40 minutes, depending on the air flow and the solutions age).
- The copper etching solution will also etch most of the silver, but some amount tends to remain adhered to the polyurethane. It can be removed by submerging the sample in a 10% nitric acid solution with Iron (III) nitrate nonahydrate (around 5 g/l), at room temperature and for 20 minutes.

## 4.9 Electrode cutting

- Load the 003 design in the MicroBeam 1.5.1.
- Using the cross in the fiduciary marks, apply four times the tool 'cut' in 'Others PU 25um' material in the MicroBeam.
- With a scalpel cut a rectangle around four electrodes, including the ACC-14 (Fig. 4.5).
- Turn the rectangle around and glue it to a microscope slide smeared with a thin layer of sugar syrup (Fig. 4.6).
- Let dry for 12 hours in a oven at 50°C.
- Remove the ACC-14 and ACC-3 films.
- Remove, very carefully, the PU around the electrodes.

## 4.10 Contac drilling

- Cut with a scalpel a rectangular area around up to 4 electrodes, without intersecting them and completely cutting both separation layers.

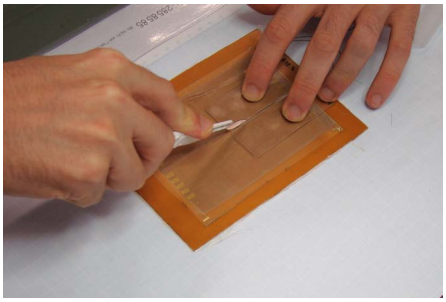

**Figure 4.5: Cut a rectangle around four electrodes** - Two microscope slides can help not to tear the PU.

a) 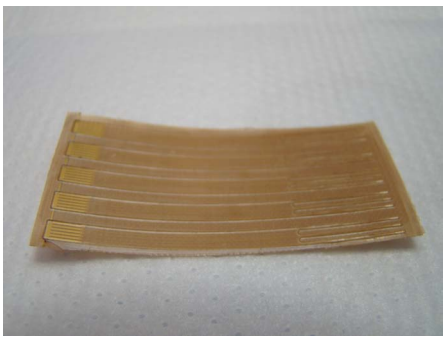 b) 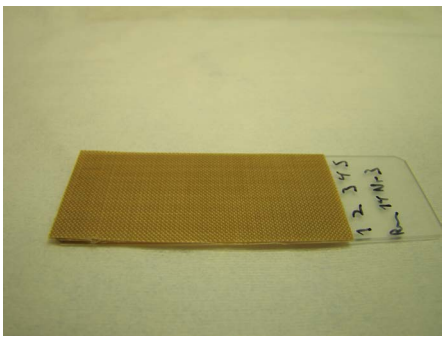

**Figure 4.6: Glue the electrodes to a microscope slide** -

- Spread sugar solution over a microscope glass slide, as thin as possible and gently press the electrodes (still with the separation layers) against the slide. Let dry for 24 hours.
- Remove the separation layers.
- Laser drill 90 $\mu$m diameter holes over the electrodes contact pads.
-

## 4.11 Contact nano-structuring

- Wet a single electrode with a tissue.
- Extract it carefully with a pair of tweezers. Should the laser cut have some partially uncut spots, cut them with a scalpel, never try pulling.

- Place the electrode on a slide with a glued PMMA piece designed for contacting.
- Contact the electrode by placing the PCB piece that also is part of the contacting system.
- Set the Gold1 bath to 50°C. Check the pH value.
- Connect all the assembly (Photo) and dip the slide until the tips of the electrode are submerged.
- Switch off the magnetic follower, leaving the hotplate on.
- Electroplate for 10 minutes with 5.4 $\mu$A.
- Wash the electrode and soak in di water for 24 hours in a fridge.
- Place the electrode over a slide with a thin layer of sugar solution, with the contacts looking upwards.
- Let dry for 24 hours in an oven at 60C.

# 5

# Conclusion

Stretchable electrodes have been succesfully built with the characteristics envisioned at the beginning of the project. The technological steps that have been found to be required are described in section 4.

Although in the previous section a method is described to produce electrode arrays according to the initial project proposal, for in vivo tests have not been conducted at the time of release of this document, it is not warranty of success in signal harvesting from nerves during chronical in vivo experiments.

Among finished electrodes, we know there is electrical connection between the nano-structured contact and the rear contact pad, because this electrical connection is used for electroplating the gold nano-crystals.

With this premise, a good enough signal-to-noise ratio would depend mainly on two factors:

- Adherence to the nerve surface, affected by growth of tissue between contact and nerve (i.e. biocompatibility).
- Conductance between electrode conductive paths, due to the permeability of PU in a physiological environment.

The first point is to be tested by another project partner, the Department of Neurology at the University of Regensburg.

For the second point, and as part of this work, a modified electrode was built, using exactly the same technological steps,

**Figure 5.1:** Finished electrode tip.

to allow easily testing the electrical behaviour of the gold electric paths embedded in PU when submerged in a physiological solution. For details see section 6.1.6. These tests suggested that the design and process proposed in this work can provide an electric resistance between adjacent conductive paths between 20 MΩ and 250 MΩ after 24 hours in a physiological solution (NaCl 0.9 molar) at room temperature. When this document was written, the causes of this differences were not known.

# 6

# Appendix

## 6.1 Experiments conducted

### 6.1.1 Gold plating thickness

These tests were performed with a X-ray spectroscopy technique used for thickness measurement of metals. In every sample 9 spots were measured, and the table shows the averages and standard deviations for each sample.

**Table 6.1:** Gold plating thickness test

| Plating time, minutes | Gold layer thickness, $\mu$m (average; standard deviation) | |
|---|---|---|
| 10 | 1.339 | 0.039 |
| 15 | 1.831 | 0.175 |
| 20 | 2.232 | 0.267 |
| 25 | 3.126 | 0.176 |
| 30 | 3.526 | 0.096 |
| 35 | 4.516 | 0.204 |

These results suggest 0.125 $\mu$m of plated gold per minute, value we used for the first calculations. Further experiments showed that these results were biased by a bad isolation of the sample's borders; the real area was bigger than measured, and the plating rate resulted to be nearer to 0.15 $\mu$m per minute.

### 6.1.2 Silver plating test

Experiment conducted to test the effects of different silver plating methods on the quality of the gold layer plated over the silver surface. Two commercial immersion silver solutions 1.2.1 were tested: MacDermid Immersion Silver and AlphaSTAR Immersion Silver. Additionally, on one sample of each solution a silver electroplating process was performed, giving a total of four combinations.

Analyzing the gold plated surface under DIC microscopy, two kinds of defects could be found:

- Dark under DIC, round shape, sometimes a particle can be seen at the middle. 20-50 $\mu$m diameter (Fig. 3.11 a and b).
- Bright under DIC, irregular shape. Up to 100 $\mu$m (Fig. 3.11 c and d).

The thickness of both the silver and gold layers was measured by x-ray spectroscopy.

**Description of the processes:** Always using copper foil with the same characteristics.

- AlphaSTAR Immersion Silver
  - 3 min Acid Cleaner at 50°C with ultrasonic vibrations.
  - 1 min Ag Microetch at 35°C.
  - 30 sec AlphaSTAR Predip at 40 °C.
  - 3 min AlphaSTAR Ag immersion at 50°C.
- MacDermid Immersion Silver.
  - 3 min Acid Cleaner at 50°C with ultrasonic vibrations.
  - 1 min Ag Microetch at 35°C.
  - 30 sec MacDermid Predip at 38 °C.
  - 2 min MacDermid Ag immersion at 52°C.
- Silver electroplating.
  - 1 min in Ag electroplating bath at room temperature. No current.
  - 2 min in Ag galvanic bath at room temperature with 52 mA ( 10 mA/cm$^2$).

**Results:**

- Test 1: AlphaSTAR Immersion Silver
  - Low concentration of both defects. Mainly bright.
  - 2.2 $\mu$m Au, 0.26 $\mu$m Ag.
- Test 2: alphaSTAR immersion silver + 2 minutes silver electroplating.
  - High concentration of bright defects.
  - 1.6 $\mu$m Au, 1.2 $\mu$m Ag.
- Test 3: MacDermid Immersion Silver.
  - High concentration of dark defects.
  - 1 $\mu$m Au, 0.42 $\mu$m Ag.
- Test 4: MacDermid Immersion Silver + 2 minutes silver electroplating.
  - High concentration of both kinds of defects.
  - 1.1 $\mu$m Au, 1.34 $\mu$m Ag.

This results let us conclude that using AlphaSTAR process alone was the only way to obtain acceptable gold plated structures on a silver plated copper foil.

### 6.1.3 AZ resist development time test

The AZ-4562 photoresist had not been previously used in Fraunhofer IZM under the conditions required by this project (i.e. a silver plated surface with features under 20 $\mu$m and avoiding waffer technology). Several tests had to be done in order to find the right parameters:

Different combinations seemed to provide good results but multiplying the energy by 2 allowed to divide the development time by 4, requiring the overall process less time. Aditionally, it was later found that the shorter the development time, the steeper the resist edeges.

**Table 6.2:** First tests with AZ development times. LDI energy = 450 mJ/cm$^2$. Prebake 10 minutes at 100°C

| Sample name | Development time, minutes | Developer concentration | Result |
|---|---|---|---|
| R6.I (13:47) | 6 | 50% | Resist rests |
| R6.II (13:44) | 8 | 50% | Resist rests |
| R6.III | 6 | 100% (old) | Resist rests |
| R6.IV | 3 | 100% | Overdeveloped |
| R6.V | 3.5 | 100% | Overdeveloped |
| R6.VI | 3.5 | 100% | Overdeveloped |
| R6.VII | 3.5 | 100% | Overdeveloped |
| R6.VIII | 3.5 | 100% | Overdeveloped |

**Table 6.3:** AZ development tests combining time and energy. Prebake 5 min at 100°C. 50% AZ developer.

| Sample name | LDI energy, mJ/cm$^2$ | Dev. time, minutes | Results |
|---|---|---|---|
| R7.A1 | 550 | 4 | Acceptable |
| R7.A2 | 600 | 3 | Acceptable |
| R7.A3 | 650 | 3 | Acceptable |
| R7.A4 | 800 | 3 | Best |
| R7.B1 | 450 | 7 | Acceptable |
| R7.B2 | 450 | 9 | Best |
| R7.B3 | 500 | 5 | Acceptable |
| R7.B4 | 550 | 4 | Acceptable |

**Table 6.4:** AZ development tests for fine adjustment of development time. LDI energy = 900 mJ/cm$^2$. Prebake 5 min at 100°C. 50% AZ developer

| Sample name | Development time | Results |
|---|---|---|
| R9.1 | 2:00 | Acceptable |
| R9.2 | 2:15 | Acceptable |
| R9.3 | 2:30 | Best |

### 6.1.4 RD 1225 test

The RD-1225 photoresist had not been used in Fraunhofer IZM, therefore we also had to perform some tests in order to find the optimal parameters: exposure energy and development time.

**Table 6.5:** RD development tests.

| Development time, minutes | LDI energy, mJ/cm$^2$ | Result |
|---|---|---|
| 3 | 25 | Fixed resist partially disolves in developer. |
| 3 | 30 | Fixed resist is stable. 30 $\mu$m holes are open. |
| 3 | 35 | Fixed resist is stable. 40 $\mu$m holes are open. |
| 6 | 30 | Fixed resist is stable. 25 $\mu$m holes are open. |
| 9 | 30 | Fixed resist is stable. 25 $\mu$m holes are open. |

30 mJ/cm$^2$ and 6 minutes of development were proved to provide the best results.

### 6.1.5 PU Laser drilling

Test performed to look for parameters to remove by laser ablation the thin layer of PU that covers the electrode contacs (see section 3.9) using the Siemens Dematic MicroBeam 3200 (see 1.5.1).

**Table 6.6:** PU laser drilling test

| Sample | Frequency, Hz | Dist. focus-surface, $\mu$m | Diameter, $\mu$m | galvospeed, mm/s |
|---|---|---|---|---|
| C1 | 4000 | 2500 | 30 | 200 |
| C2 | 4000 | 2500 | 5 punches | 200 |
| C3 | 5000 | 1000 | 20 | 200 |
| C4 | 4000 | 2000 | 20 | 200 |
| C5 | 4000 | 1500 | 10 | 200 |
| C6 | 4000 | 1500 | 10 | 100 |

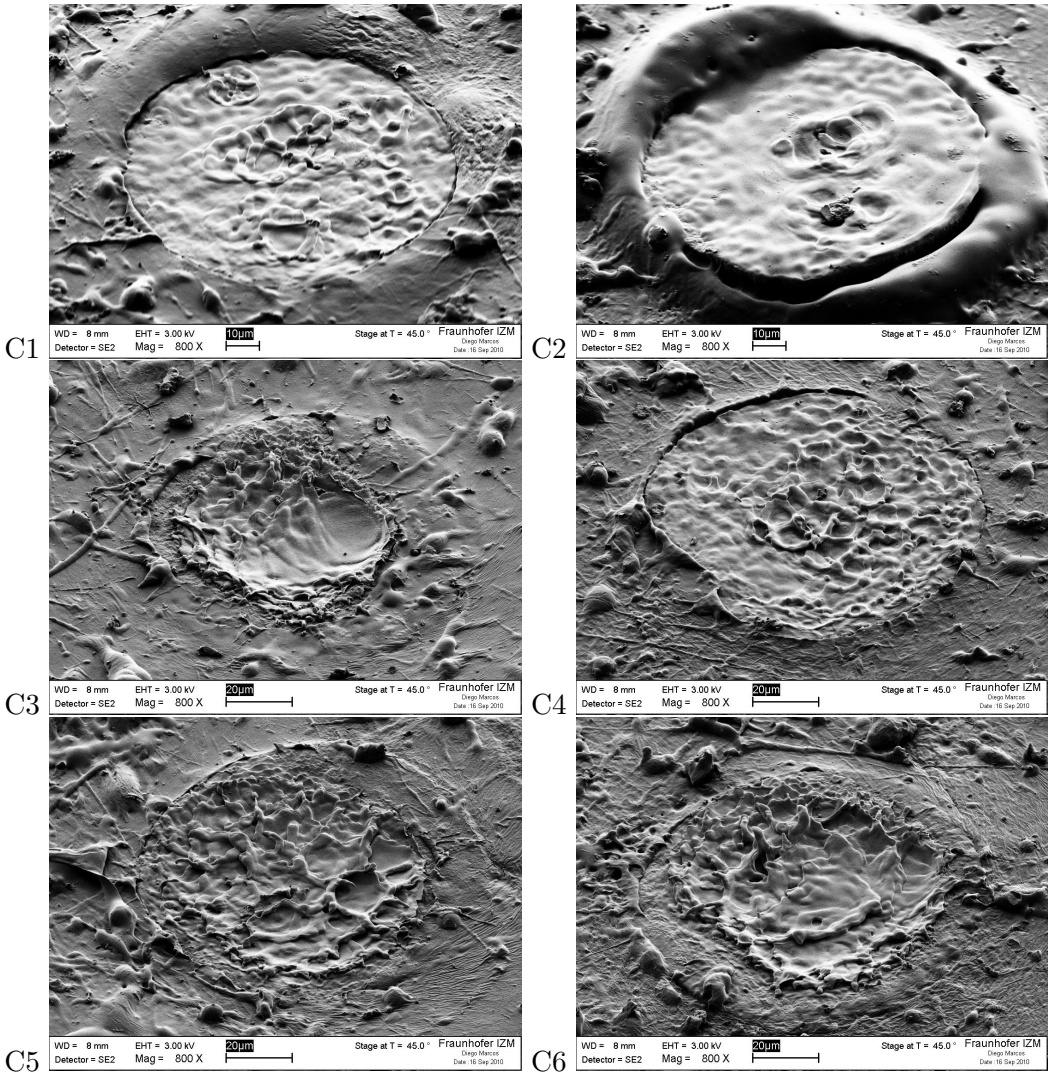


**Figure 6.1: Results of the PU drilling test** - C1 was selected as the best parameter collection. SEM images.

### 6.1.6 Behaviour in physiological solution

Using the same process explained in section 4, samples were built to perform conductance tests in physiological solution, aimed to verify in what range lies the isolation provided by the PU embedding. These samples (Fig. 6.2) consist of two conductive paths, with the same meander shape as the ones used for the electrode arrays, running parallel for a distance of 5 cm. Both extremes of each path are accesible through a

contact pad. The four contact pads are at one side of the sample, to allow dipping the conductive paths in a physiological solution.

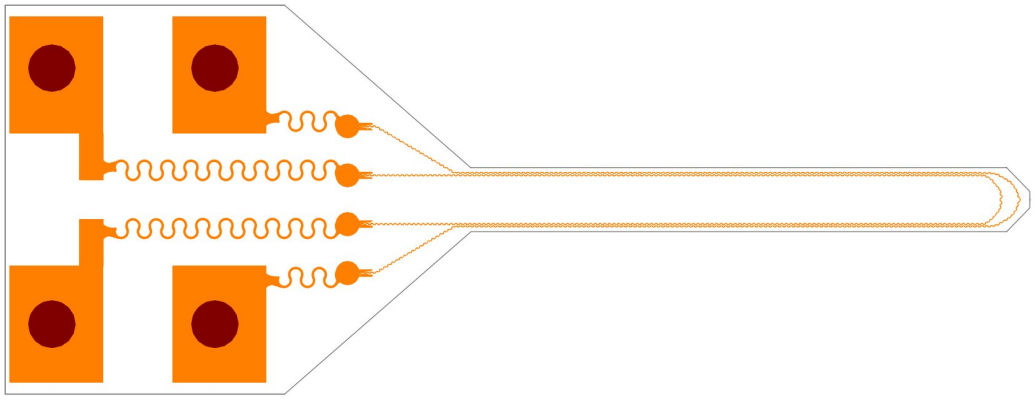

**Figure 6.2: Detail of a sample to test behaviour in physiological solution** - Orange is the main gold electroplating step, red the contact reinforcement and gray the final shape of the sample, cut by laser.

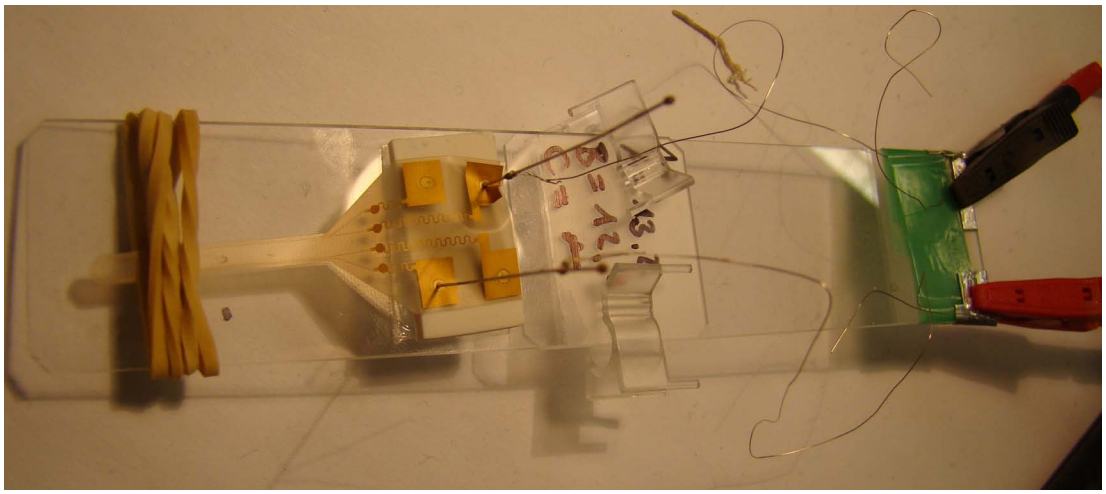

**Figure 6.3: Sample prepared for a test** - The lower 1 cm of the sample will be dipped in a NaCl 0.9% solution.

Several tests were performed, exposing 2 cm of the meander shaped parallel conductive paths to NaCl 0.9% solution. The device used to measure the resistance between paths was a Keithley 2001, able to measure up to 1 GOhm, and the data was collected

using a program written in MATLAB. The results tended to be irregular the first 5 hours and stabilize afterwards (Fig. 6.4), remaining constant for the 2 weeks the test was run. This final value was found to vary from sample to sample, but being always in the range 20 - 250 MOhm. Distance between paths seems to have a bigger role than expected, and reducing in a 50% this distance seems to increase by 500% the conductivity between paths, but other parameters could be involved, like conductive residues after etching or partial PU delamination(19).

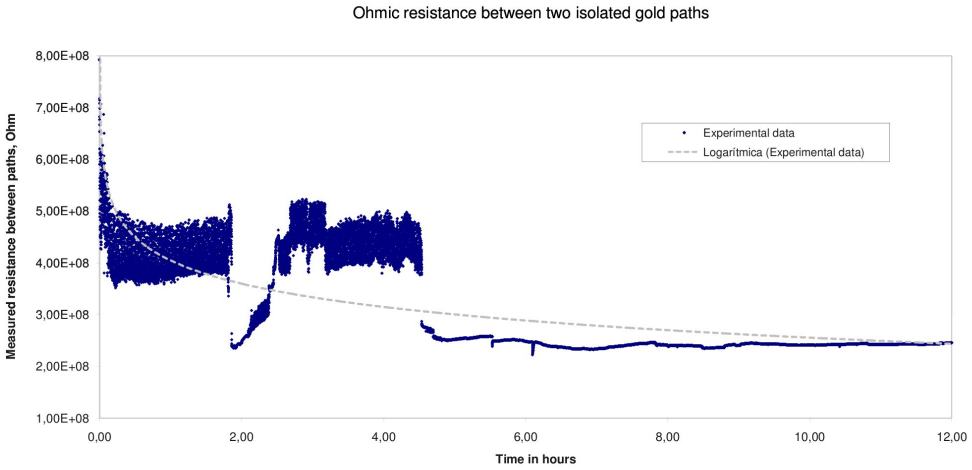


**Figure 6.4: Resistance measured in a sample with 180 $\mu$m distance between paths for a period of 12 hours** - For the first 5 hours the values jump in the range 250 - 500 MOhm. After 5 hours, it stabilizes around 250 MOhm.

### 6.1.7 Dark layer spectroscopy

The samples that had been handeled with GoldStripper 645 tend to show a strange behaviour after etching the copper and silver away: the PU was covered by a dark layer with high levels of electrical conductivity. Different methods where unsuccesfully tried to remove this layer, most under the assumption that it consisted of some kind of silver compound embedded in the PU:

- Rubbing under water: works but damages the PU.
- $HNO_3$ with iron (III) nitrate: nothing happens.
- HCl in various concentrations: nothing happens.
- $NH_3$ in various concentrations: nothing happens.
- Reduce with aluminum foil in a $NaHCO_3$ bath for 12 hours: oxidation occured in the aluminum, but the layer over the PU was not affected.

After these experiments, we started to think that the dark layer did not consist of silver compounds. We decided to analyze a PU sample under EDX, what showed an important presence of gold micro-particles embedded in the PU (Figs. 6.56.66.7). It was confirmed after observing how this dark layer would disappear after 5 seconds in contact with GoldStripper 645.

Project 1 - Sample 1

01.03.2010 18:01:11

Spectrum processing :
No peaks omitted

Processing option : All elements analyzed
(Normalised)
Number of iterations = 2

Standard :
C CaCO3 1-Jun-1999 12:00 AM
O SiO2 1-Jun-1999 12:00 AM
Ag Ag 1-Jun-1999 12:00 AM
Au Au 1-Jun-1999 12:00 AM

Comment:
Pr4-run8, PU-OF nach Cu-Ätzen

| Element | Weight% | Atomic% |
|---|---|---|
| C K | 24.83 | 79.05 |
| O K | 0.00 | 0.00 |
| Ag L | 39.65 | 14.05 |
| Au M | 35.52 | 6.89 |
| Totals | 100.00 | |

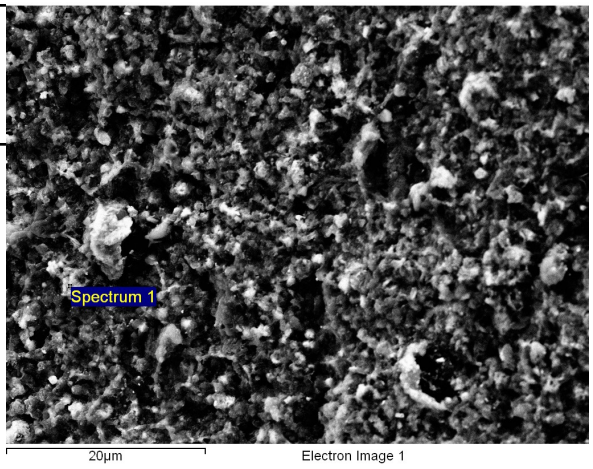


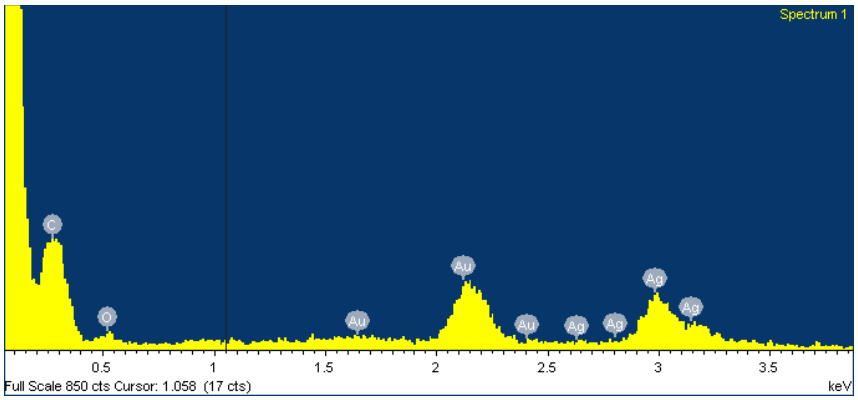


**Figure 6.5: PU conductive layer EDX test spot 1** - 35% of gold in weight in the area where a conductive particle can be seen.

Project 1 - Sample 1

01.03.2010 18:00:37

Spectrum processing :
No peaks omitted

Processing option : All elements analyzed
(Normalised)
Number of iterations = 2

Standard :
C CaCO3 1-Jun-1999 12:00 AM
O SiO2 1-Jun-1999 12:00 AM
Ag Ag 1-Jun-1999 12:00 AM
Au Au 1-Jun-1999 12:00 AM

Comment:
Pr4-run8, PU-OF nach Cu-Ätzen

| Element | Weight% | Atomic% |
|---|---|---|
| C K | 82.60 | 98.22 |
| O K | 0.00 | 0.00 |
| Ag L | 8.59 | 1.14 |
| Au M | 8.80 | 0.64 |
| Totals | 100.00 | |

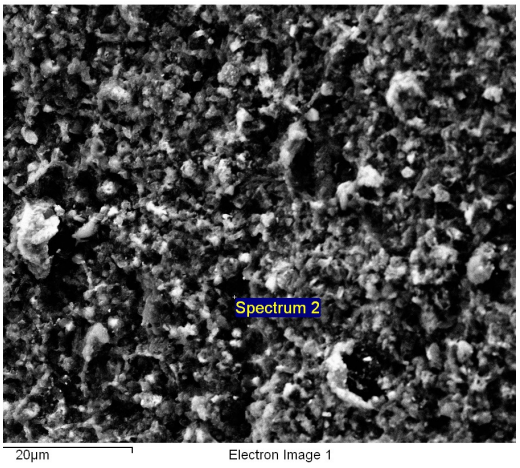


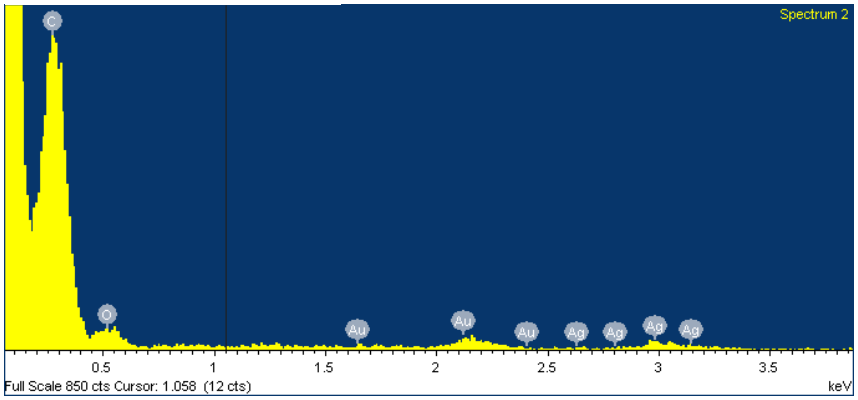


**Figure 6.6: PU conductive layer EDX test spot 2** - 8% of gold in weight in the area mostly consisting of organic material.

Project 1 - Sample 1

01.03.2010 17:58:52

Spectrum processing :
No peaks omitted

Processing option : All elements analyzed (Normalised)
Number of iterations = 2

Standard :
C CaCO3 1-Jun-1999 12:00 AM
O SiO2 1-Jun-1999 12:00 AM
Ag Ag 1-Jun-1999 12:00 AM
Au Au 1-Jun-1999 12:00 AM

Comment:
Pr4-run8, PU-OF nach Cu-Ätzen

| Element | Weight% | Atomic% |
|---|---|---|
| C K | 46.20 | 90.32 |
| O K | 0.00 | 0.00 |
| Ag L | 33.15 | 7.22 |
| Au M | 20.65 | 2.46 |
| Totals | 100.00 | |

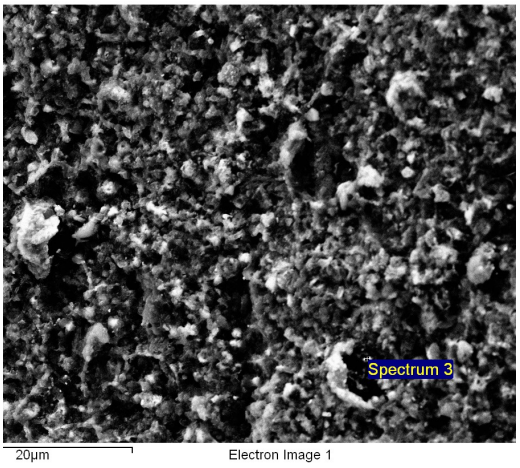


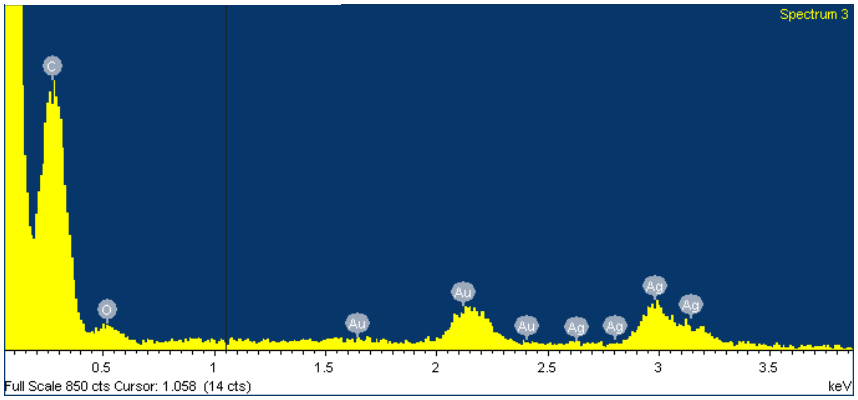


**Figure 6.7: PU conductive layer EDX test spot 3** - 20% of gold in weight in the area where a conductive particle can be seen

## 6.2 Drawings

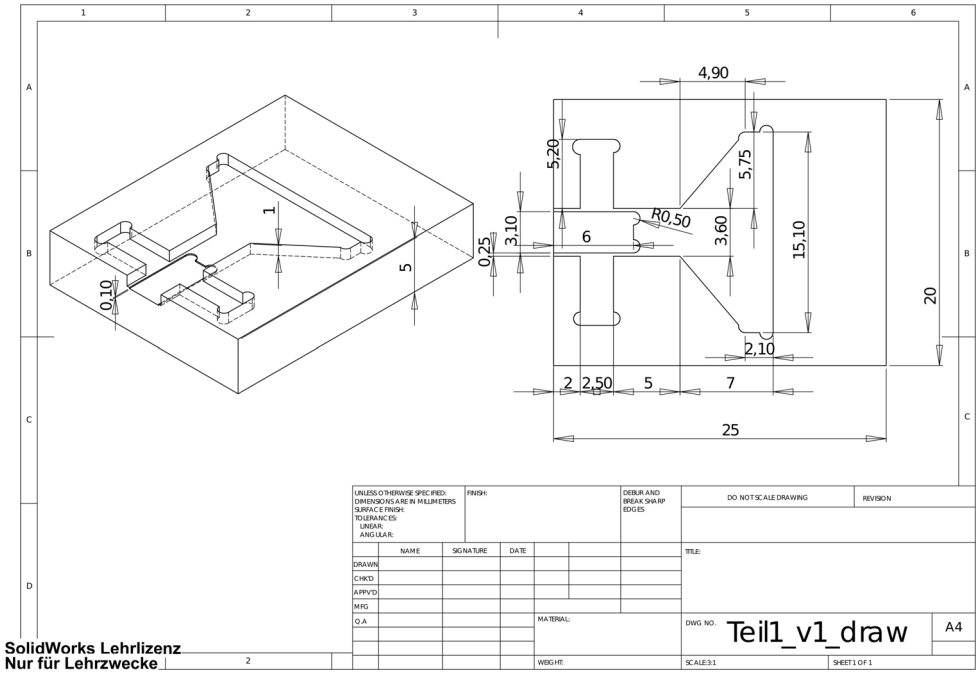


**Figure 6.8: SolidWorks design for the PMMA piece of the contacting clamp -**

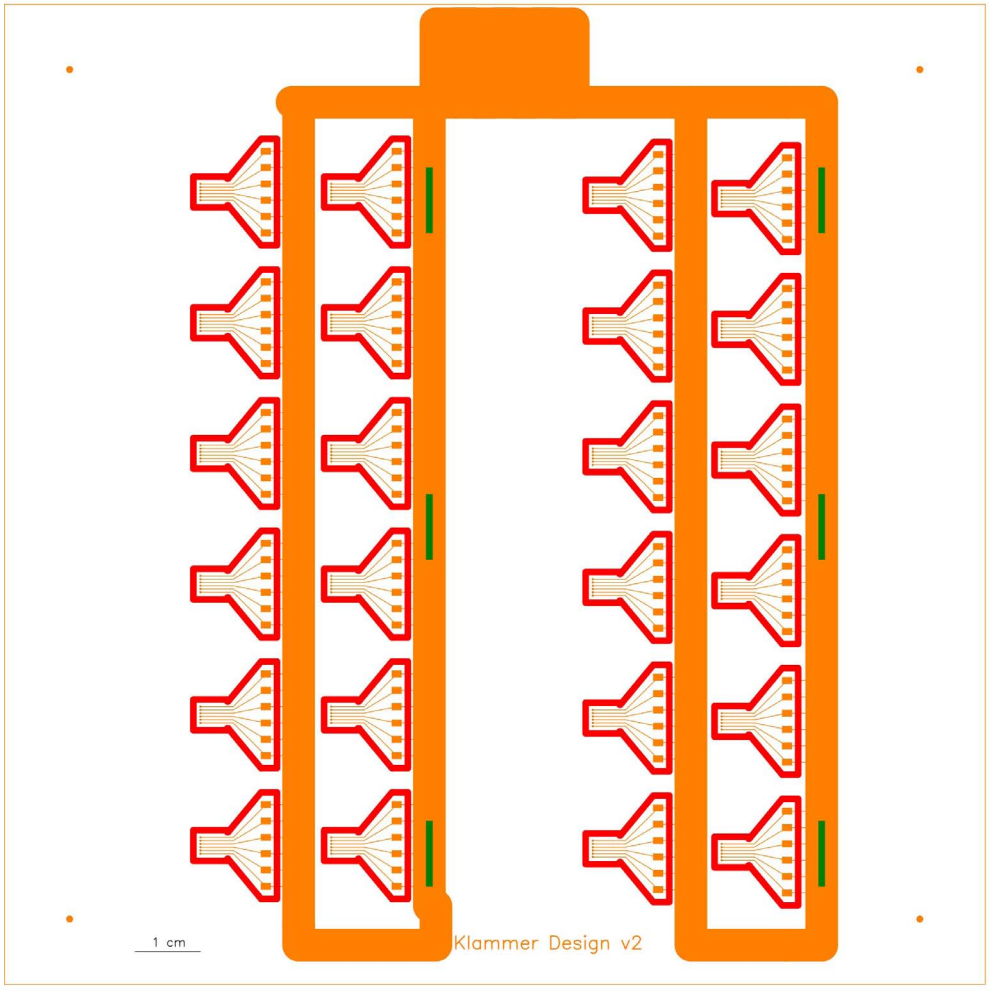


**Figure 6.9: CAM 350 desing for the PCB piece of the contacting clamp -**

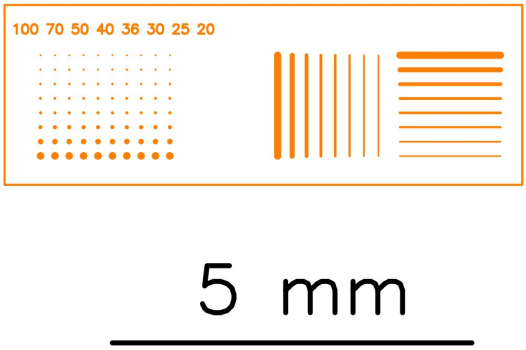


**Figure 6.10: Design used for photoresist tests -**

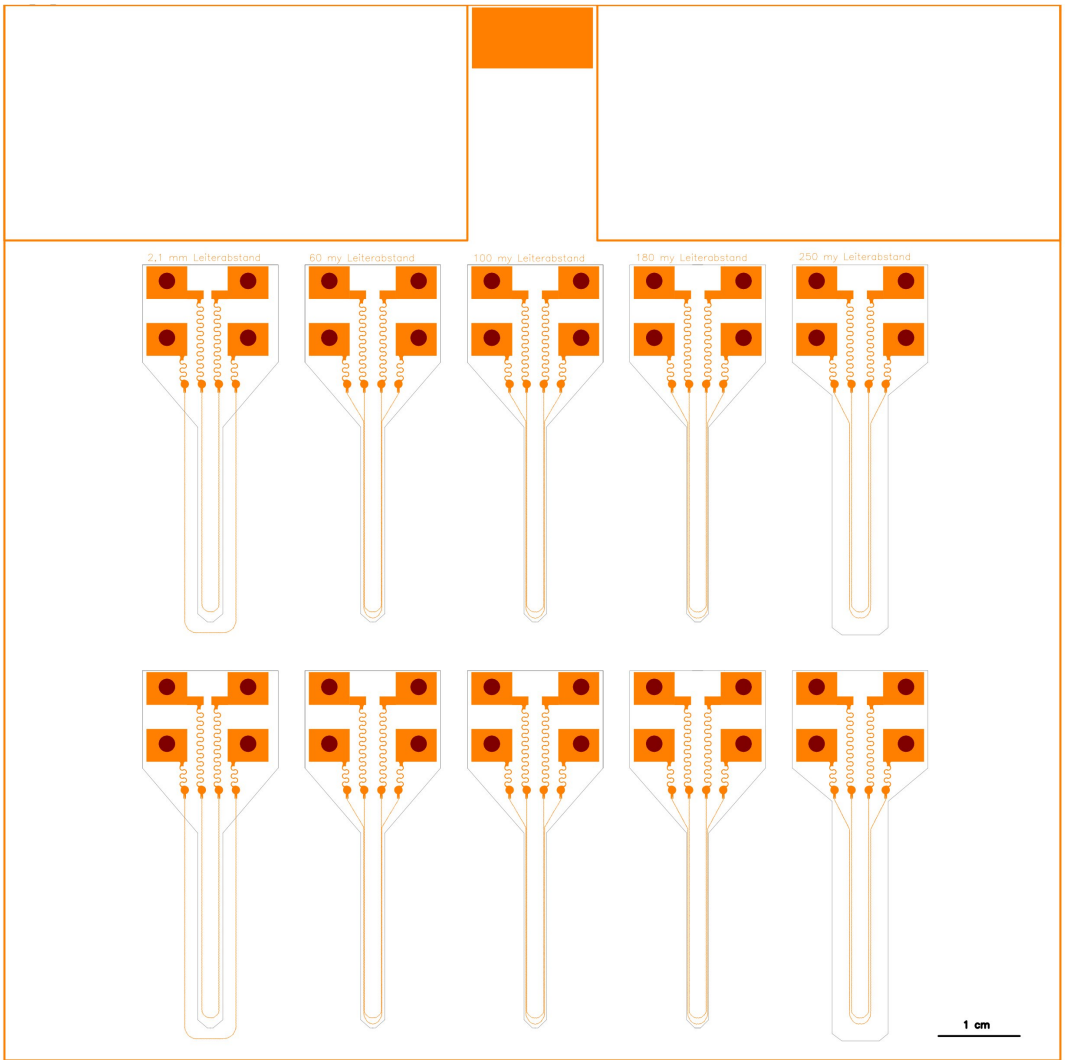


**Figure 6.11: Layout of the samples to test behaviour in physiological solution -**

# List of Figures

# List of Tables

# Glossary

**DIC microscopy** Differential interference contrast microscopy, an optical microscopy illumination technique used to enhance the contrast in unstained samples.

**EDX** Energy-dispersive X-ray spectroscopy, an analytical technique used for the elemental analysis or chemical characterization of a sample.

**FR-4** Glass reinforced epoxy laminate sheet.

**PCB** Printed Circuit Board.

**PMMA** Poly(methyl methacrylate).

**PTFE** polytetrafluoroethylene, commonly known with the brand name Teflon.

**PU** Polyurethane, a high resilient and flexible polymere consisting of a chain of organic units joined by urethane (carbamate) links.

**Thief** An auxiliary cathode so placed as to divert to itself some current from portions of the article which would otherwise receive too high a current density. (20)

# References


[1] **http://www.gesundheitsforschung-bmbf.de/de/451.php**. 1

[2] Chang-Hsiao Chen et al. **Micro-multi-probe electrode array to measure neural signals**. *Biosensors and Bioelectronics*, **24**:1911–1917, 2009. 1

[3] Karen C. Cheung et al. **Flexible polyimide microelectrode array for in vivo recordings and current source density analysis**. *Biosensors and Bioelectronics*, **22**:1783–1790, 2007. 1

[4] S. Hirsch and C. Rosenstein. *Metal Finishing 65th Guidebook*, chapter Immersion Plating, page 424. M. Murphy, ed., 1997. 3

[5] P. Wilkinson. **Understanding Gold Plating**. *Gold Bulletin*, **19 (3)**, 1986. 3

[6] Marc J. Madou. *Fundamentals of Microfabrication*. M. Murphy, ed., Florida, 1997. 5

[7] S. Bitzer and P. van der Smagt. **IEEE International Conference on Robotics and Automation**. In *Learning EMG control of a robotic hand: towards active prostheses*, pages 2819–2823, 2006. 5

[8] Richard F. et al. **Implantable Myoelectric Sensors (IMESs) for Intramuscular Electromyogram Recording**. *IEEE Transactions on Biomedical Engineering*, **56 (1)**, 2009. 5

[9] B. Blankertz et al. **The non-invasive Berlin Brain-Computer Interface**. *Neuroimage*, **37 (2)**:539–550, 2007. 6

[10] E. Niedermeyer and F. Lopes da Silva. *Electroencephalography: Basic Principles, Clinical Applications, and Related Fields*. Lippincot, 2004. 6

[11] M.D. Serruya and J.P. Donoghue. *Design Principles of a Neuromotor Prosthetic Device in Neuroprosthetics*. Imperial College Press, 2003. 6

[12] **http://www.stella-project.de**. 6

[13] A. Ostmann et al. **International Conference on Electronic Materials and Packaging**. In *Manufacturing Concepts for Stretchable Electronic Systems*, 2008. 6

[14] Sunchana P. Pucic. **Instrumentation and Measurement Technology Conference**. In *Diffusion of Copper into Gold Plating*, 1993. 19

[15] Robert Wm. Cooke. *Red Plague Control Plan*. NASA - Johnson Space Center. 20

[16] Lars Boettcher et al. **Microsystems, Packaging, Assembly and Circuits Technology Conference**. In *Embedding of Chips for System in Package realization*, 2008. 24

[17] Several. *Process Guidelines for Alkaline Etching*. Chemcut Corp., 2002. 37

[18] Craighead et al. **Modification for Control of Central Nervous System Cells**. *Biomedical Microdevices*, **1 (1)**:49–64, 1998. 42

[19] O. van der Sluis et al. **Analysis of the three-dimensional delamination behavior of stretchable electronics applications**. *Key Engineering Materials*, **417-418**:9–12, 2009. 72

[20] **http://www.letsfinishit.com/plateglossary.htm**. 86

# Declaration

I herewith declare that I have produced this document without the prohibited assistance of third parties and without making use of aids other than those specified; notions taken over directly or indirectly from other sources have been identified as such. This document has not previously been presented in identical or similar form to any other Spanish or foreign examination board.

The thesis work was conducted from November 2009 to February 2011 under the supervision of Michael Zwanzig at Fraunhofer IZM.

BERLIN, February 2011